units), SDH3, SDH4, and SDH8–SDH11 (hydrophobic subunits) (Table 2). All subunits, except SDH1-1, are trypanosomatid-specific and structurally unrelated to plant-specific soluble subunits (AtSDH5–AtSDH8, 5–18 kDa) (27–29). All genes (except SDH6 with four copies) are present as two copies, which are assigned to either Esmeraldo or non-Esmeraldo haplotype (haploid genotype) in *T. cruzi* subgroup IIe. In contrast, only one copy each of the orthologues is present in *T. brucei*, *Leishmania major*, *Leishmania infantum*, and *Leishmania braziliensis* (supplemental Table S1). N-terminal sequence analysis of SDH3 and SDH7 showed that yields of two isoforms are similar (*i.e.* SDH3-1:SDH3-2 = 63:37, and SDH7-1:SDH7-2 = 54:46), indicating that isoforms are expressed from each haplotype. Because truncated isoforms for SDH1 and SDH5 in the Esmeraldo haplotype (see below) are not assembled into the 12-subunit complex and $SDH2_N$ and SDH9 isoforms have the identical sequence, 512 ($= 1^4 \times 4^1 \times 2^{(12-5)}$) kinds of heterogeneity may exist in the *T. cruzi* Complex II monomer (Table 2).

Flavoprotein Subunit—SDH1-1 (63-kDa band in Tricine-PAGE) cross-reacted with the antiserum against bovine SDH1 (data not shown) and is highly homologous to counterparts in *T. brucei* (93% identity), *L. major* (90%), *Homo sapiens* (59%), *Arabidopsis thaliana* (62%), *Saccharomyces cerevisiae* (61%), and *Escherichia coli* (48%, SdhA). Amino acid residues proposed for dicarboxylate binding and a FAD ligand histidine (12–14) are all conserved in SDH1-1. SDH1-1 and SDH5-1 of the non-Esmeraldo haplotype share a weak sequence similarity in the entire region, but the latter lacks amino acid residues responsible for FAD and dicarboxylate binding. In the Esmeraldo haplotype, SDH1-2 and SDH5-2 are truncated and contain only Met^1 to Gly^{167} of TcSDH1-1 and Ile^{305} to Met^{486} of TcSDH5-1, respectively (Table 2). These findings suggest that TcSDH1-1, TcSDH1-2, TcSDH5-1, and TcSDH5-2 might have evolved by gene duplication and subsequent degeneration.

Iron-Sulfur Subunit—Sequence analysis of the 25- and 21-kDa band proteins revealed that they contain the plant ferredoxin domain (Ip_N) and bacterial ferredoxin domain (Ip_C) of canonical SDH2 (Ip) in the N- and C-terminal half, respectively (Fig. 4). Sequence identities of Ip_N and Ip_C are 37 and 43%, respectively, to those of human SDH2 (Table 2), and the Ip_N and Ip_C domains contain all amino acid residues responsible for binding of iron-sulfur clusters and ubiquinone (12, 13, 30) (Fig. 4). Such a heterodimeric Ip subunit can be found in *T. brucei* (31), *T. cruzi*, *L. major*, *L. infantum*, and *L. braziliensis* (Tables 2), which belong to the order Trypanosomatida. Thus we named these subunits as $SDH2_N$ and $SDH2_C$, respectively.

Splitting of mitochondrial membrane proteins has been reported for cytochrome *c* oxidase CoxII in Apicomplexa and Chlorophyceae (32, 33), and ATP synthase α subunit in *Leishmania tarentolae* and *T. brucei* (34, 35). The former occurs at the gene level and the latter by post-translational cleavage. Sequence analysis indicates that heterodimeric SDH2 and CoxII have emerged from gene duplication followed by degeneration of the N- or C-terminal half of the duplication products. Conserved domains in degenerated duplicons, which have arisen from mitochondrion-to-nucleus transfer of the duplicated genes (32, 33, 36), must retain the potential for protein-protein interactions and constitute a heterodimeric functional subunit by trans-complementation.

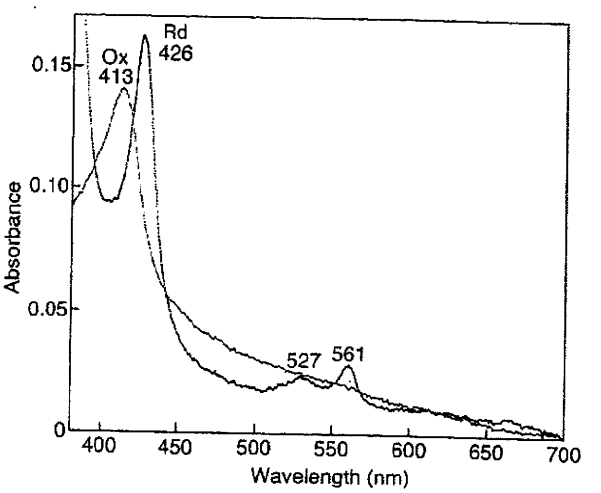

FIGURE 6. **Visible absorption spectra of *T. cruzi* Complex II.** Purified Complex II was desalted by ultrafiltration and diluted with 0.1 M sodium phosphate, pH 7.2, containing 0.1% SML at a final concentration of 0.06 mg/ml. Absorption spectra of the air-oxidized (*Ox, thin line*) and dithionite-reduced (*Rd, thick line*) forms were recorded at room temperature with UV-2400 spectrophotometer (Shimadzu Corp., Kyoto, Japan).

Membrane Anchor Subunits—Membrane anchor subunits in protist enzymes are highly divergent from bacterial and mammalian counterparts and difficult to find with conventional BLAST programs. We identified candidates for *T. cruzi* SDH3 and SDH4 by the presence of the quinone/heme-binding motifs "$RPX_{16}SX_2HR$ (SDH3 helix I)" and "$HX_{10}DY$ (SDH4 helix V)," respectively, present in membrane anchor subunits. In Complex II, Trp^{164} in SDH2 (Fig. 4) and Tyr^{83} in the SDH4 $HX_{10}DY$ motif (Fig. 5*B*) (*E. coli* numbering) could hydrogen bond to the O-1 atom of ubiquinone and contribute to the binding affinity (12, 37). Arg^{31} in the SDH3 SX_2HR motif (Fig. 5*A*) and Asp^{82} in the SDH4 $HX_{10}DY$ motif are in close proximity to ubiquinone and could interact with Tyr^{83} (37). Ser^{27} in the SDH3 SX_2HR motif has been shown to be essential for quinone binding (38) and is a candidate for hydrogen bonding to the O-4 atom of ubiquinone (30). The first arginine (Arg^9 in *E. coli* SDH3) in the $RPX_{16}SX_3R$ motif is in the vicinity of Glu^{186} in SDH1 and Asp^{106} in SDH2 and may play a structural role by making a hydrogen bond network.

In *T. cruzi*, SDH3 has the "$RPX_{11}SX_2HR$ motif in front of the predicted transmembrane helix I and lacks transmembrane helices II and III. However, sequence alignment suggests the presence of the alternative motif "$TX_2SR/(T)$" in the Trypanosomatida (Fig. 5*A*). In mitochondrial Complex II, protoheme IX is ligated by two His residues in the second transmembrane helix of SDH3 ("$HX_{10}D$" motif) and SDH4 ("$HX_{10}DY$" motif). A heme ligand in helix II (His^{84} in *E. coli* SDH3) may be substituted by a nearby histidine in the quinone-binding motif "SX_2HR" (39). In contrast, SDH4 lacks helix IV and appears to interact with heme and ubiquinone with the $HX_{10}DY$ motif. As in rice SDH4 (GenBank™ accession number NP_001045324), the heme ligand His is substituted by Gln in *T. brucei* SDH4. The presence of a bound heme or an alternative ligand in *T.*

brucei SDH4 needs to be tested in future studies. It is also possible that trypanosomatid-specific subunits could be assembled as a jigsaw puzzle-like membrane anchor.

Spectroscopic Properties of T. cruzi Complex II—Pyridine ferrohemochrome analysis showed that *T. cruzi* Complex II binds a stoichiometric amount of protoheme IX (0.85 heme/monomer of enzyme) indicating that monomer enzyme complex contains one heme. At room temperature, the air-oxidized and fully reduced forms of the purified enzyme showed peaks at 413 and 426, 527, and 561 nm, respectively (Fig. 6). Peak positions are similar to those reported for Complex II from *E. coli* (40), adult *A. suum* (41), and bovine (42, 43), where heme is ligated via histidine in the second helices of SDH3 and SDH4. Although heme has an important role in the assembly of Complex II, it is not essential for the reduction of ubiquinones (43, 44).

Enzymatic Properties of T. cruzi Complex II—We examined SQR activity of the purified enzyme and found the difference in apparent K_m values between Q_1 (33.9 ± 3.6 μM) and Q_2 (18.8 ± 6.4 μM) (Fig. 7), indicating that the 6-polyprenyl group of ubiquinone contributes to the binding affinity. The apparent V_{max} value of the *T. cruzi* Complex II was rather constant, 11.9 ± 2.2 for Q_1 and 11.5 ± 0.4 Q_2 units/mg proteins, respectively, and one-fourth of those reported for bovine and *E. coli* enzymes (45, 46). This is not surprising because *T. cruzi* complex II has about 2–3 times more proteins than the other enzymes. K_m values for ubiquinone and succinate (18.8 ± 6.4 μM (Q_2) and 1.48 ± 0.17 mM, respectively) were higher than 0.3 and 130 μM, respectively, of bovine enzyme (45), and 2 and 277 μM, respectively, of the *E. coli* enzyme (46, 47). Notably, the K_m value for succinate was comparable with 610 μM in adult *A. suum* (10), which expresses the stage-specific Complex II as quinol:fumarate reductase under hypoxic habitats in host organisms.

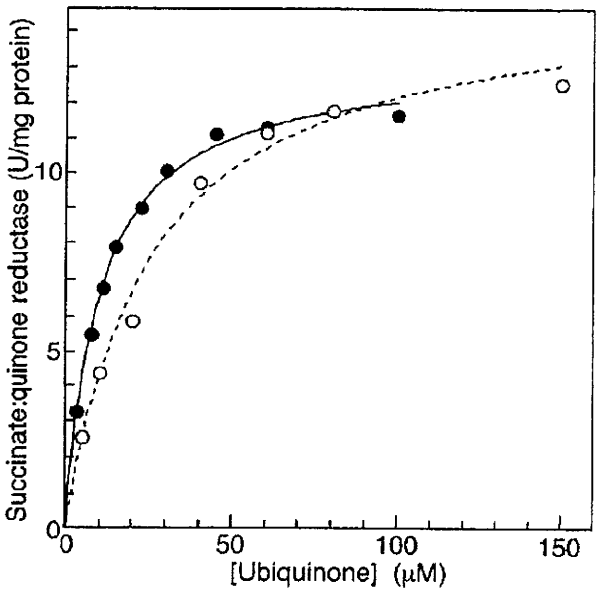

FIGURE 7. **Kinetic analysis of succinate-quinone reductase activity.** Succinate:ubiquinone reductase activity of the purified Complex II was determined with Q_1 (○) and Q_2 (●) at a protein concentration of 1.25 μg/ml in the presence of 10 mM sodium succinate. Data were fitted with the Michaelis-Menten equation using KaleidaGraph, and apparent K_m and V_{max} values were 30.3 ± 4.3 μM and 14.0 ± 1.2 units/mg protein, respectively, for Q_1 and 12.4 ± 0.7 μM and 11.9 ± 0.3 units/mg protein, respectively, for Q_2.

Then we examined effects of inhibitors for binding sites of quinones and dicarboxylates on SQR activity. Atpenin A5, a potent inhibitor for Complex II, inhibited the *T. cruzi* enzyme with the IC_{50} value of 6.4 ± 2.4 μM, which is 3 orders of magnitude higher than that of bovine Complex II (4 nM) (48). Furthermore, carboxin, 2-theonyltrifluoroacetone, plumbagin, and 2-heptyl-4-hydroxyquinoline *N*-oxide were ineffective (100 μM $<IC_{50}$). Structural divergence in trypanosomatid SDH3 and SDH4 could be the cause for lower binding affinities for both quinones and inhibitors. In addition, we found for the dicarboxylate-binding site that the IC_{50} value for malonate (40 μM) was much higher than the K_i value for bovine Complex II (1.3 μM) (45).

Structure of Trypanosomatid Complex II—To the best of our knowledge, this is the first report on the isolation of protist Complex II. *T. cruzi* Complex II has unusual subunit organization with six each of hydrophilic and hydrophobic subunits. Such a supramolecular structure and heterodimeric SDH2 ($SDH2_N$ and $SDH2_C$) are conserved in the Trypanosomatida. Furthermore, SDH1, $SDH2_N$, $SDH2_C$, SDH3, SDH4, and SDH8–SDH10 can be identified in the ongoing genome projects on the evolutionary relatives, the photosynthetic free-living *Euglena gracilis*, and the nonphotosynthetic euglenoid *Astasia longa* in the Euglenida. Thus a part of these features are common in the Euglenozoa, a divergent lineage of eukaryotes (Fig. 8).

Accumulation of noncatalytic subunits through expanding the protein interaction network could be a driving force for protein evolution. Structural and catalytic features are unique, and thus this enzyme could be a potential target for novel chemotherapeutic agents for trypanosomiasis and leishmaniasis.

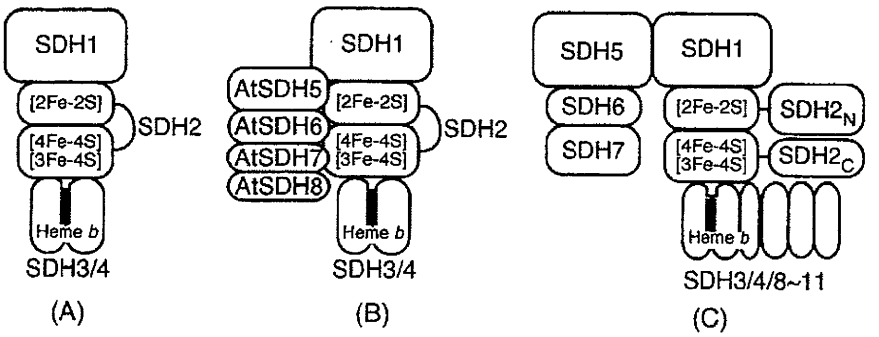

FIGURE 8. **Subunit organization of Complex II.** *A*, common four-subunit Complex II (*e.g.* mammals, *E. coli*); *B*, eight-subunit Complex II in plants (*e.g. A. thaliana*); and *C*, 12-subunit Complex II in the Trypanosomatida. Noncatalytic subunits and domains are shown in *yellow* and heme in *red*.

Conclusion—The parasitic protist *T. brucei* is a gold mine where unprecedented biological phenomena like RNA editing and trans-splicing in mitochondria were originally discovered. It was found recently in *Diplonema papillatum*, a free-living evolutionary cousin,

that mature mRNA for cytochrome *c* oxidase CoxI was assembled from nine gene fragments by a jigsaw puzzle mechanism (49). From a characterization of Complex II from *T. cruzi*, we revealed a novel supramolecular organization, which is conserved in the Trypanosomatida.

Parasites have exploited unique energy metabolic pathways as adaptations to their natural habitats within their hosts (50, 51). In fact, the respiratory systems of parasites typically show greater diversity in electron transfer pathways than those of host animals. As shown in this study, such is also the case with Complex II, which is a well known marker enzyme of mitochondria. Studies on the role of supramolecular Complex II in adaptation of trypanosomatids is now underway in our laboratory.

Acknowledgments—We thank Drs. J. L. Concepcion (Universidad de Los Andes, Merida-Venezuela) and T. Nara (Juntendo University) for kind advice; and Drs. M. Matsuzaki (University of Tokyo), T. Hashimoto (University of Tsukuba), G. Cecchini (University of California San Francisco), and M. Müller (Rockefeller University) for critical reading of the manuscript.

REFERENCES

1. World Health Organization (2007) *Report of the First Meeting of WHO Strategic and Technical Advisory Group on Neglected Tropical Diseases*, pp. 1–26, Geneva, Switzerland
2. Berriman, M., Ghedin, E., Hertz-Fowler, C., Blandin, G., Renauld, H., Bartholomeu, D. C., Lennard, N. J., Caler, E., Hamlin, N. E., Haas, B., Bohme, U., Hannick, L., Aslett, M. A., Shallom, J., Marcello, L., Hou, L., Wickstead, B., Alsmark, U. C., Arrowsmith, C., Atkin, R. J., Barron, A. J., Bringaud, F., Brooks, K., Carrington, M., Cherevach, I., Chillingworth, T. J., Churcher, C., Clark, L. N., Corton, C. H., Cronin, A., Davies, R. M., Doggett, J., Djikeng, A., Feldblyum, T., Field, M. C., Fraser, A., Goodhead, I., Hance, Z., Harper, D., Harris, B. R., Hauser, H., Hostetler, J., Ivens, A., Jagels, K., Johnson, D., Johnson, J., Jones, K., Kerhornou, A. X., Koo, H., Larke, N., Landfear, S., Larkin, C., Leech, V., Line, A., Lord, A., Macleod, A., Mooney, P. J., Moule, S., Martin, D. M., Morgan, G. W., Mungall, K., Norbertczak, H., Ormond, D., Pai, G., Peacock, C. S., Peterson, J., Quail, M. A., Rabbinowitsch, E., Rajandream, M. A., Reitter, C., Salzberg, S. L., Sanders, M., Schobel, S., Sharp, S., Simmonds, M., Simpson, A. J., Tallon, L., Turner, C. M., Tait, A., Tivey, A. R., Van Aken, S., Walker, D., Wanless, D., Wang, S., White, B., White, O., Whitehead, S., Woodward, J., Wortman, J., Adams, M. D., Embley, T. M., Gull, K., Ullu, E., Barry, J. D., Fairlamb, A. H., Opperdoes, F., Barrell, B. G., Donelson, J. E., Hall, N., Fraser, C. M., Melville, S. E., and El-Sayed, N. M. (2005) *Science* **309**, 416–422
3. Cazzulo, J. J. (1994) *J. Bioenerg. Biomembr.* **26**, 157–165
4. Besteiro, S., Barrett, M. P., Riviere, L., and Bringaud, F. (2005) *Trends Parasitol.* **21**, 185–191
5. Bringaud, F., Riviere, L., and Coustou, V. (2006) *Mol. Biochem. Parasitol.* **149**, 1–9
6. Takashima, E., Inaoka, D. K., Osanai, A., Nara, T., Odaka, M., Aoki, T., Inaka, K., Harada, S., and Kita, K. (2002) *Mol. Biochem. Parasitol.* **122**, 189–200
7. Van Hellemond, J. J., Opperdoes, F. R., and Tielens, A. G. (1998) *Proc. Natl. Acad. Sci. U. S. A.* **95**, 3036–3041
8. Harington, J. S. (1961) *Parasitology* **51**, 309–318
9. Roos, M. H., and Tielens, A. G. (1994) *Mol. Biochem. Parasitol.* **66**, 273–281
10. Saruta, F., Kuramochi, T., Nakamura, K., Takamiya, S., Yu, Y., Aoki, T., Sekimizu, K., Kojima, S., and Kita, K. (1995) *J. Biol. Chem.* **270**, 928–932
11. Cecchini, G. (2003) *Annu. Rev. Biochem.* **72**, 77–109
12. Yankovskaya, V., Horsefield, R., Tornroth, S., Luna-Chavez, C., Miyoshi, H., Leger, C., Byrne, B., Cecchini, G., and Iwata, S. (2003) *Science* **299**, 700–704
13. Sun, F., Huo, X., Zhai, Y., Wang, A., Xu, J., Su, D., Bartlam, M., and Rao, Z. (2005) *Cell* **121**, 1043–1057
14. Huang, L. S., Sun, G., Cobessi, D., Wang, A. C., Shen, J. T., Tung, E. Y., Anderson, V. E., and Berry, E. A. (2006) *J. Biol. Chem.* **281**, 5965–5972
15. El-Sayed, N. M., Myler, P. J., Bartholomeu, D. C., Nilsson, D., Aggarwal, G., Tran, A. N., Ghedin, E., Worthey, E. A., Delcher, A. L., Blandin, G., Westenberger, S. J., Caler, E., Cerqueira, G. C., Branche, C., Haas, B., Anupama, A., Arner, E., Aslund, L., Attipoe, P., Bontempi, E., Bringaud, F., Burton, P., Cadag, E., Campbell, D. A., Carrington, M., Crabtree, J., Darban, H., da Silveira, J. F., de Jong, P., Edwards, K., Englund, P. T., Fazelina, G., Feldblyum, T., Ferella, M., Frasch, A. C., Gull, K., Horn, D., Hou, L., Huang, Y., Kindlund, E., Klingbeil, M., Kluge, S., Koo, H., Lacerda, D., Levin, M. J., Lorenzi, H., Louie, T., Machado, C. R., McCulloch, R., McKenna, A., Mizuno, Y., Mottram, J. C., Nelson, S., Ochaya, S., Osoegawa, K., Pai, G., Parsons, M., Pentony, M., Pettersson, U., Pop, M., Ramirez, J. L., Rinta, J., Robertson, L., Salzberg, S. L., Sanchez, D. O., Seyler, A., Sharma, R., Shetty, J., Simpson, A. J., Sisk, E., Tammi, M. T., Tarleton, R., Teixeira, S., Van Aken, S., Vogt, C., Ward, P. N., Wickstead, B., Wortman, J., White, O., Fraser, C. M., Stuart, K. D., and Andersson, B. (2005) *Science* **309**, 409–415
16. Ivens, A. C., Peacock, C. S., Worthey, E. A., Murphy, L., Aggarwal, G., Berriman, M., Sisk, E., Rajandream, M. A., Adlem, E., Aert, R., Anupama, A., Apostolou, Z., Attipoe, P., Bason, N., Bauser, C., Beck, A., Beverley, S. M., Bianchettin, G., Borzym, K., Bothe, G., Bruschi, C. V., Collins, M., Cadag, E., Ciarloni, L., Clayton, C., Coulson, R. M., Cronin, A., Cruz, A. K., Davies, R. M., De Gaudenzi, J., Dobson, D. E., Duesterhoeft, A., Fazelina, G., Fosker, N., Frasch, A. C., Fraser, A., Fuchs, M., Gabel, C., Goble, A., Goffeau, A., Harris, D., Hertz-Fowler, C., Hilbert, H., Horn, D., Huang, Y., Klages, S., Knights, A., Kube, M., Larke, N., Litvin, L., Lord, A., Louie, T., Marra, M., Masuy, D., Matthews, K., Michaeli, S., Mottram, J. C., Muller-Auer, S., Munden, H., Nelson, S., Norbertczak, H., Oliver, K., O'Neil, S., Pentony, M., Pohl, T. M., Price, C., Purnelle, B., Quail, M. A., Rabbinowitsch, E., Reinhardt, R., Rieger, M., Rinta, J., Robben, J., Robertson, L., Ruiz, J. C., Rutter, S., Saunders, D., Schafer, M., Schein, J., Schwartz, D. C., Seeger, K., Seyler, A., Sharp, S., Shin, H., Sivam, D., Squares, R., Squares, S., Tosato, V., Vogt, C., Volckaert, G., Wambutt, R., Warren, T., Wedler, H., Woodward, J., Zhou, S., Zimmermann, W., Smith, D. F., Blackwell, J. M., Stuart, K. D., Barrell, B., and Myler, P. J. (2005) *Science* **309**, 436–442
17. Bourguignon, S. C., Mello, C. B., Santos, D. O., Gonzalez, M. S., and Souto-Padron, T. (2006) *Acta Trop.* **98**, 103–109
18. Concepcion, J. L., Chataing, B., and Dubourdieu, M. (1999) *Comp. Biochem. Physiol.* **122**, 211–222
19. Matsudaira, P. (1987) *J. Biol. Chem.* **262**, 10035–10038
20. Rosenfeld, J., Capdevielle, J., Guillemot, J. C., and Ferrara, P. (1992) *Anal. Biochem.* **203**, 173–179
21. Brusca, J. S., and Radolf, J. D. (1994) *Methods Enzymol.* **228**, 182–193
22. Wittig, I., Karas, M., and Schagger, H. (2007) *Mol. Cell. Proteomics* **6**, 1215–1225
23. Sabar, M., Balk, J., and Leaver, C. J. (2005) *Plant J.* **44**, 893–901
24. Berry, E. A., and Trumpower, B. L. (1987) *Anal. Biochem.* **161**, 1–15
25. Larkin, M. A., Blackshields, G., Brown, N. P., Chenna, R., McGettigan, P. A., McWilliam, H., Valentin, F., Wallace, I. M., Wilm, A., Lopez, R., Thompson, J. D., Gibson, T. J., and Higgins, D. G. (2007) *Bioinformatics (Oxf.)* **23**, 2947–2948
26. Schagger, H., and Pfeiffer, K. (2000) *EMBO J.* **19**, 1777–1783
27. Millar, A. H., Eubel, H., Jansch, L., Kruft, V., Heazlewood, J. L., and Braun, H. P. (2004) *Plant Mol. Biol.* **56**, 77–90
28. Eubel, H., Heinemeyer, J., and Braun, H. P. (2004) *Plant Physiol.* **134**, 1450–1459
29. Eubel, H., Heinemeyer, J., Sunderhaus, S., and Braun, H. P. (2004) *Plant Physiol. Biochem.* **42**, 937–942
30. Horsefield, R., Yankovskaya, V., Sexton, G., Whittingham, W., Shiomi, K., Omura, S., Byrne, B., Cecchini, G., and Iwata, S. (2006) *J. Biol. Chem.* **281**, 7309–7316
31. Allen, J. W., Ginger, M. L., and Ferguson, S. J. (2004) *Biochem. J.* **383**, 537–542
32. Funes, S., Davidson, E., Reyes-Prieto, A., Magallon, S., Herion, P., King, M. P., and Gonzalez-Halphen, D. (2002) *Science* **298**, 2155

33. Waller, R. F., and Keeling, P. J. (2006) *Gene (Amst.)* **383,** 33–37
34. Williams, N., and Frank, P. H. (1990) *Mol. Biochem. Parasitol.* **43,** 125–132
35. Nelson, R. E., Aphasizheva, I., Falick, A. M., Nebohacova, M., and Simpson, L. (2004) *Mol. Biochem. Parasitol.* **135,** 221–224
36. Adams, K. L., Rosenblueth, M., Qiu, Y. L., and Palmer, J. D. (2001) *Genetics* **158,** 1289–1300
37. Tran, Q. M., Rothery, R. A., Maklashina, E., Cecchini, G., and Weiner, J. H. (2006) *J. Biol. Chem.* **281,** 32310–32317
38. Yang, X., Yu, L., He, D., and Yu, C. A. (1998) *J. Biol. Chem.* **273,** 31916–31923
39. Maklashina, E., Rothery, R. A., Weiner, J. H., and Cecchini, G. (2001) *J. Biol. Chem.* **276,** 18968–18976
40. Kita, K., Vibat, C. R., Meinhardt, S., Guest, J. R., and Gennis, R. B. (1989) *J. Biol. Chem.* **264,** 2672–2677
41. Takamiya, S., Furushima, R., and Oya, H. (1986) *Biochim. Biophys. Acta* **848,** 99–107
42. Tushurashvili, P. R., Gavrikova, E. V., Ledenev, A. N., and Vinogradov, A. D. (1985) *Biochim. Biophys. Acta* **809,** 145–159
43. Tran, Q. M., Rothery, R. A., Maklashina, E., Cecchini, G., and Weiner, J. H. (2007) *Proc. Natl. Acad. Sci. U. S. A.* **104,** 18007–18012
44. Oyedotun, K. S., Sit, C. S., and Lemire, B. D. (2007) *Biochim. Biophys. Acta* **1767,** 1436–1445
45. Grivennikova, V. G., Gavrikova, E. V., Timoshin, A. A., and Vinogradov, A. D. (1993) *Biochim. Biophys. Acta* **1140,** 282–292
46. Maklashina, E., and Cecchini, G. (1999) *Arch. Biochem. Biophys.* **369,** 223–232
47. Miyadera, H., Hiraishi, A., Miyoshi, H., Sakamoto, K., Mineki, R., Murayama, K., Nagashima, K. V., Matsuura, K., Kojima, S., and Kita, K. (2003) *Eur. J. Biochem.* **270,** 1863–1874
48. Miyadera, H., Shiomi, K., Ui, H., Yamaguchi, Y., Masuma, R., Tomoda, H., Miyoshi, H., Osanai, A., Kita, K., and Omura, S. (2003) *Proc. Natl. Acad. Sci. U. S. A.* **100,** 473–477
49. Marande, W., and Burger, G. (2007) *Science* **318,** 415
50. Kita, K., and Takamiya, S. (2002) *Adv. Parasitol.* **51,** 95–131
51. Tielens, A. G., Rotte, C., van Hellemond, J. J., and Martin, W. (2002) *Trends Biochem. Sci.* **27,** 564–572
52. Krogh, A., Larsson, B., von Heijne, G., and Sonnhammer, E. L. L. (2001) *J. Mol. Biol.* **305,** 567–580
53. Mitaku, S., Hirokawa, T., and Tsuji, T. (2002) *Bioinformatics* **18,** 608–616

Acta Crystallographica Section F
Structural Biology and Crystallization Communications
ISSN 1744-3091

Crystallization of mitochondrial rhodoquinol-fumarate reductase from the parasitic nematode *Ascaris suum* with the specific inhibitor flutolanil

Arihiro Osanai,[a] Shigeharu Harada,[b] Kimitoshi Sakamoto,[a]* Hironari Shimizu,[a] Daniel Ken Inaoka[a] and Kiyoshi Kita[a]

[a]Department of Biomedical Chemistry, Graduate School of Medicine, University of Tokyo, 7-3-1 Hongo, Bunkyo-ku, Tokyo 113-0033, Japan, and [b]Department of Applied Biology, Graduate School of Science and Technology, Kyoto Institute of Technology, Sakyo-ku, Kyoto 606-8585, Japan

Correspondence e-mail: sakamok@m.u-tokyo.ac.jp

Received 2 June 2009
Accepted 8 August 2009

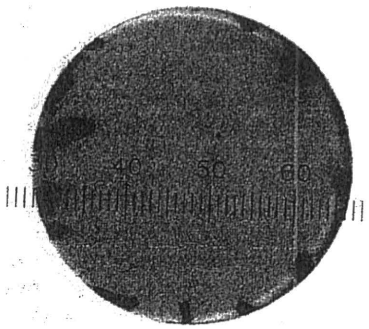

In adult *Ascaris suum* (roundworm) mitochondrial membrane-bound complex II acts as a rhodoquinol-fumarate reductase, which is the reverse reaction to that of mammalian complex II (succinate-ubiquinone reductase). The adult *A. suum* rhodoquinol-fumarate reductase was crystallized in the presence of octaethyleneglycol monododecyl ether and *n*-dodecyl-β-D-maltopyranoside in a 3:2 weight ratio. The crystals belonged to the orthorhombic space group $P2_12_12_1$, with unit-cell parameters $a = 123.75$, $b = 129.08$, $c = 221.12$ Å, and diffracted to 2.8 Å resolution using synchrotron radiation. The presence of two molecules in the asymmetric unit (120 kDa × 2) gives a crystal volume per protein mass (V_M) of 3.6 Å^3 Da^{-1}.

1. Introduction

In parasites, fumarate plays an important role in redox homeostasis. The parasitic protozoan *Trypanosoma cruzi* utilizes bacterial-type dihydroorotate dehydrogenase (TcDHOD), which is the fourth enzyme in the pyrimidine-biosynthesis pathway and catalyzes the oxidation of dihydroorotate and the reduction of fumarate to succinate. We have elucidated the catalytic mechanisms of these sequential reactions by determination of the three-dimensional structures of TcDHOD in the ligand-free form and in complex with the substrates (dihydroorotate and fumarate), product (orotate and succinate) and inhibitor (oxonate) at atomic resolution (Inaoka *et al.*, 2008).

In parasitic helminths, fumarate is the terminal electron acceptor of the anaerobic respiratory chain, which is essential for the survival of the parasites in the host (Kita & Takamiya, 2002). Complex II catalyzes fumarate reduction in anaerobic respiration and functions as a terminal oxidase. In eukaryotes, complex II (succinate-ubiquinone reductase in aerobic respiration; SQR) is located in the inner mitochondrial membrane and is generally composed of four polypeptides. The flavoprotein (Fp) subunit is the largest, with an approximate molecular mass of 70 kDa, and contains flavin adenine dinucleotide (FAD) as a prosthetic group. Complex II contains a relatively hydrophilic catalytic region formed by the Fp subunit and an iron–sulfur cluster (Ip) subunit, which has a molecular mass of approximately 30 kDa. The remaining subunits comprise cytochrome *b*, which contains a haem *b*. Cytochrome *b* is composed of two hydrophobic membrane-anchoring polypeptide subunits, namely a 15 kDa large subunit (CybL) and a 13 kDa small subunit (CybS). These cytochrome *b* subunits are necessary for the interaction of complex II with hydrophobic membrane-associated quinones such as ubiquinone (UQ) and rhodoquinone (RQ).

Our recent study on the respiratory chain of the parasitic nematode *Ascaris suum* has shown that the mitochondrial NADH-fumarate reductase system plays an important role in the anaerobic energy metabolism of adult parasites inhabiting hosts and that they undergo unique developmental changes during their life cycle (Kita & Takamiya, 2002; Iwata *et al.*, 2008). In anaerobic metabolism by *A. suum* mitochondria, the transfer of a reducing equivalent from NADH to the low-potential RQ is conducted by the NADH–RQ reductase complex (complex I). This pathway ends with the production of succinate by the rhodoquinol-fumarate reductase (QFR) activity of complex II. Electron transfer from NADH to fumarate is

coupled to site I phosphorylation of complex I *via* the generation of a proton gradient. The difference in redox potential between the NAD^+/NADH couple (E'_m = −320 mV) and the fumarate/succinate couple (E'_m = +30 mV) is sufficient to drive ATP synthesis.

The anaerobic NADH-fumarate reductase system is found not only in nematodes but also in bacteria and many other parasites and is a promising target for chemotherapy (Omura *et al.*, 2001; Tielens *et al.*, 2002; Matsumoto *et al.*, 2008). The most potent inhibitor of complex II, atpenin A5, was found during screening for inhibitors of *A. suum* complex II (Miyadera *et al.*, 2003). However, the mammalian complex II is much more sensitive to atpenin A5 than the *A. suum* enzyme. By further screening, we have found that flutolanil, a commercially available fungicide (Ito *et al.*, 2004), specifically inhibits the *A. suum* complex II. Therefore, we have taken flutolanil as a lead compound for structure-based drug design. In the current study, we have purified, crystallized and performed preliminary X-ray diffraction studies on the adult *A. suum* QFR.

2. Methods

2.1. Purification

Mitochondria were prepared from the muscle of adult *A. suum* as described by Takamiya *et al.* (1984), except that Chappell–Perry medium (100 m*M* KCl, 50 m*M* Tris–HCl pH 7.4, 1 m*M* ATP, 5 m*M* $MgSO_4$ and 1 m*M* EDTA; Ernster & Nordenbrand, 1967) was used instead of MSE medium (210 m*M* mannitol, 70 m*M* sucrose and 0.1 m*M* EDTA). The QFR was solubilized from adult *A. suum* mitochondria in 1.0%(*w*/*v*) sucrose monolaurate (Dojindo) and purified in the presence of 0.1%(*w*/*v*) sucrose monolaurate. *A. suum* mitochondria (1 g protein) were homogenized in 500 ml buffer *A* (10 m*M* Tris–HCl pH 7.5, 1 m*M* sodium malonate) containing 1.0%(*w*/*v*) sucrose monolaurate. After incubating the mixture for 30 min at 277 K, it was centrifuged for 1 h at 200 000*g*. The clear reddish-brown supernatant containing the solubilized QFR was applied onto a GE Healthcare DEAE Sepharose FF column (2.6 × 24 cm) pre-equilibrated with buffer *A* containing 0.1%(*w*/*v*) sucrose monolaurate. After washing the column with the same buffer, the QFR was eluted with 2400 ml of the buffer containing a linear gradient of 0.0–0.3 *M* NaCl. Fractions containing the QFR, which started to elute at approximately 0.1 *M* NaCl, were pooled and adjusted to 0.15 g ml^{-1} polyethylene glycol 3350 (Hampton Research) to precipitate the QFR. The mixture was centrifuged for 20 min at 15 000*g* and the precipitate was dissolved in buffer *A* containing 0.1%(*w*/*v*) sucrose monolaurate. The QFR was then further loaded onto a GE Healthcare Source 15Q column (1.6 × 10 cm) and eluted with 400 ml of buffer containing a linear gradient of 0–0.3 *M* NaCl. Fractions containing pure QFR as judged by SDS–PAGE (Fig. 1) were pooled. The purified QFR was then precipitated by adding solid polyethylene glycol (PEG) 3350 to 0.15 g ml^{-1} and stored at 193 K.

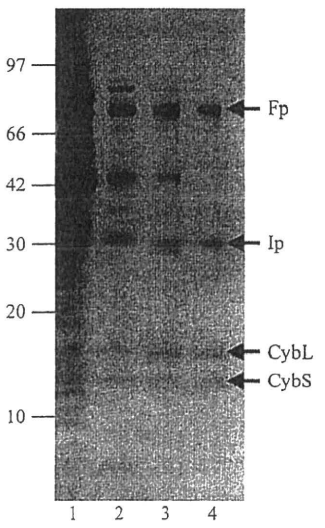

Figure 1
Purity of *A. suum* QFR at different stages of purification. Samples were separated by SDS–PAGE and the gel was stained with Coomassie Blue. The positions of molecular-weight markers are indicated on the left (in kDa) and the four subunits of *A. suum* QFR (Fp, flavoprotein subunit; Ip, iron–sulfur cluster subunit; CybL, cytochrome *b* large subunit; CybS, cytochrome *b* small subunit) are labelled on the right. Lane 1, whole mitochondria; lane 2, supernatant obtained after ultracentrifugation of the detergent extract; lane 3, pooled fractions from the DEAE Sepharose FF column; lane 4, pooled fractions from the Source 15Q column.

2.2. Crystallization

Conditions for crystallizing the *A. suum* QFR were screened using Crystal Screen (Jancarik & Kim, 1991) and Crystal Screen II (Hampton Research). Crystallization by hanging-drop vapour diffusion was carried out using 96-well CrystalClear Strips (Hampton Research). A droplet containing equal volumes of approximately 20 mg ml^{-1} QFR in buffer *A* containing detergent and reservoir solution was equilibrated against 100 µl reservoir solution.

Aggregates of microcrystals were observed at 293 K from reservoir solutions containing polyethylene glycols with medium molecular weights and 200 m*M* salts when octaethyleneglycol monododecyl ether (C12E8) was used as a detergent. Attempts to optimize the conditions by altering the PEG type (3350, 4000 and 6000), PEG concentration and pH and by using Additive Screen kits (Hampton Research) did not succeed in improving the crystallization. We therefore examined the effect of adding another detergent as an additive. 0.1 volume of detergent solution was added to a droplet of approximately 20 mg ml^{-1} QFR in buffer *A* containing 0.5%(*w*/*v*) C12E8 and an equal volume of reservoir solution and crystallization by hanging-drop vapour diffusion was carried out. After several days, small crystals (~10 µm; Fig. 2*a*) appeared at 293 K in drops from reservoir solutions composed of 14–18%(*w*/*v*) PEG 3350, 100 m*M* Tris–HCl pH 7.5–8.6, 200 m*M* NaCl and 1 m*M* sodium malonate when the drops included 0.3–0.5%(*w*/*v*) *n*-dodecyl-β-D-maltopyranoside (C12M). To determine the optimal ratio of C12E8 to C12M, crystallization was carried out using QFR dissolved in buffer *A* containing different concentrations of C12E8 and C12M. The best condition for crystallization (Fig. 2*b*) was achieved at a 3:2 C12E8:C12M weight ratio.

Crystals larger than 100 µm in size were grown by the microdialysis method as follows. The precipitate of the purified QFR stored at 193 K was dissolved in buffer *A* (approximately 10 mg ml^{-1}) containing 0.6%(*w*/*v*) C12E8, 0.4%(*w*/*v*) C12M and 200 m*M* NaCl. After incubation for 20 min on ice, the QFR was precipitated by adding an equal volume of 40%(*w*/*v*) PEG 3350. The precipitate obtained by centrifugation was dissolved in the same buffer, incubated for 20 min on ice and mixed with an equal volume of 40%(*w*/*v*) PEG 3350 to precipitate the QFR. This procedure was repeated several times in order to replace sucrose monolaurate with the added detergent. The precipitate was finally dissolved in buffer *A* containing 0.06%(*w*/*v*) C12E8, 0.04%(*w*/*v*) C12M and 0.2 *M* NaCl, giving an approximately 40 mg ml^{-1} QFR solution. After adding an equal volume of 23%(*w*/*v*) PEG 3350 to the QFR solution, undissolved materials were removed by centrifugation for 20 min at 20 000*g*. The supernatant was then sealed in a 5 µl microdialysis button and dialyzed against

reservoir solution containing 15.0%(*w*/*v*) PEG 3350, 100 m*M* Tris–HCl pH 8.4, 200 m*M* NaCl, 1 m*M* sodium malonate, 0.06%(*w*/*v*) C12E8 and 0.04%(*w*/*v*) C12M. Dark red plate-shaped crystals appeared within 24 h and grew to 100–200 µm after 2–3 d at 293 K (Fig. 2*c*).

X-ray diffraction data were collected on BL44XU at SPring-8 (Harima, Japan) and on BL-5A and NW12A at the Photon Factory (Tsukuba, Japan) by the rotation method. For X-ray diffraction experiments at 100 K, a QFR crystal mounted on a nylon loop was transferred successively to reservoir solution supplemented with 3.75, 7.5, 11.25 and 15% glycerol and was then frozen by rapid submergence in liquid nitrogen. Data were processed and scaled using *HKL*-2000 and *SCALEPACK* (Otwinowski & Minor, 1997).

3. Results and discussion

To obtain sufficient *A. suum* mitochondria for purification of the QFR, we slightly modified the standard protocol. Specifically, we used Chappell–Perry medium (Ernster & Nordenbrand, 1967) in place of the standard medium. This resulted in 0.95 mg mitochondria per gram of muscle and 0.3 µmol min^{-1} mg^{-1} mitochondrial succinate dehydrogenase activity, which represents a threefold increase in recovery and a fourfold increase in specific activity compared with the previous method (Takamiya *et al.*, 1984). Using this method, we obtained 7.5 mg pure enzyme (Fig. 1, lane 4) from 1 kg of adult *A. suum* muscle.

Because the success of membrane-protein crystallization strongly depends on which detergent is used, we tested a variety of commercially available nonionic detergents in the screening of crystallization conditions for the *A. suum* QFR. Aggregates of microcrystals were obtained under several crystallization conditions using the detergent C12E8, but we were unable to optimize the conditions. Instead, the optimal condition for producing crystals suitable for X-ray structure analysis was achieved when the sucrose monolaurate was exchanged for a 3:2 weight ratio of C12E8:C12M (Fig. 2*c*). Crystals grew to larger than 100 µm in 2–3 d by dialyzing QFR, which was dissolved in buffer *A* containing 11.5%(*w*/*v*) PEG 3350, 0.06%(*w*/*v*) C12E8, 0.04%(*w*/*v*) C12M and 200 m*M* NaCl, against reservoir solution containing 15.0%(*w*/*v*) PEG 3350, 100 m*M* Tris–HCl pH 8.4, 200 m*M* NaCl, 1 m*M* sodium malonate, 0.06%(*w*/*v*) C12E8 and 0.04%(*w*/*v*) C12M. Adding 11.5%(*w*/*v*) PEG 3350 to the QFR solution in advance prevented serious bubble formation in the microdialysis button, which was unfavourable for crystallization.

X-ray diffraction patterns were recorded from a single crystal at 100 K with an oscillation angle of 1.0° using a Bruker DIP-6040 imaging-plate detector on the BL44XU beamline at SPring-8. Analysis of the symmetry and the systematic absences in the recorded diffraction pattern indicated that the crystals belonged to the orthorhombic space group $P2_12_12_1$, with unit-cell parameters a = 123.75, b = 129.08, c = 221.12 Å. Assuming the presence of two QFR molecules (120 kDa × 2) in the asymmetric unit, the calculated Matthews coefficient V_M (Matthews, 1968) was 3.6 $Å^3$ Da^{-1}. A total of 587 189 observed reflections recorded on 180 images were merged to 75 372 unique reflections from 50.0 to 2.8 Å resolution.

During the screening of inhibitors, we found that flutolanil (Ito *et al.*, 2004), a commercially available fungicide, specifically inhibits *A. suum* SQR. The IC_{50} of flutolanil against *A. suum* and bovine SQR was 0.081 and 16 µ*M*, respectively, indicating that flutolanil is a promising lead compound for anthelminthics. To enable rational drug optimization, we prepared crystals of the *A. suum* QFR complexed with flutolanil by the soaking method. X-ray diffraction patterns were recorded at 100 K on 130 frames with an oscillation angle of 1° using an ADSC Quantum 315 CCD detector on NW12 at Photon Factory. A total of 54 964 unique reflections from 50.0 to 3.2 Å resolution were obtained. The data-collection and processing statistics are summarized in Table 1.

We attempted to solve the structure of the *A. suum* QFR by the molecular-replacement method using the *MOLREP* program (Navaza, 1994) as implemented within *CCP*4 (Collaborative Computational Project, Number 4, 1994) and the refined coordinates

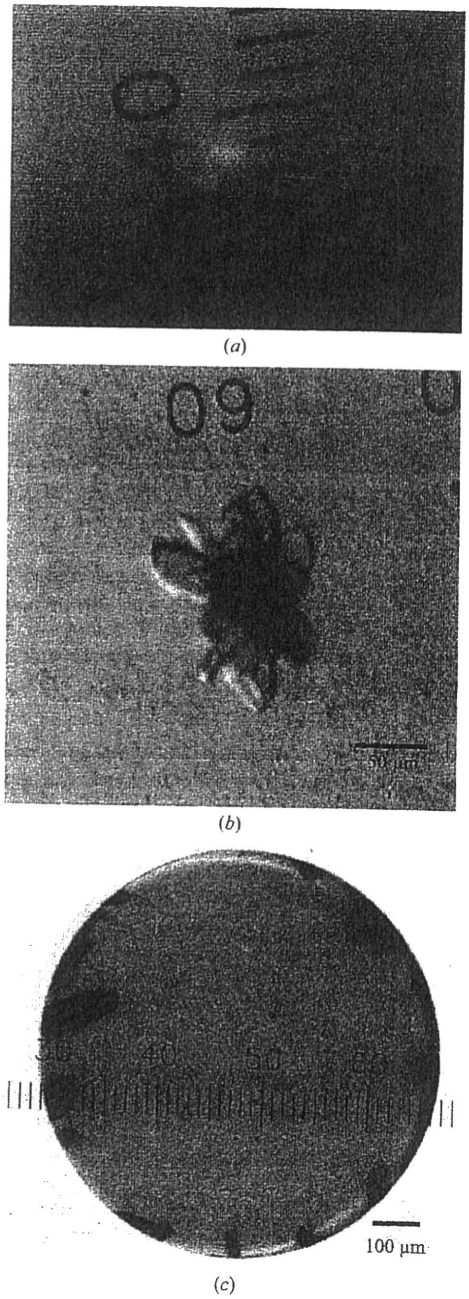

(*a*)

(*b*)

(*c*)

Figure 2
Typical crystals of *A. suum* QFR. Crystals of *A. suum* QFR obtained (*a*) by the hanging-drop vapour-diffusion method using C12E8 as the main detergent and C12M as the additive detergent, (*b*) using a 3:2 weight ratio of C12E8 and C12M and (*c*) after detergent exchange to the 3:2 C12E8:C12M mixture by microdialysis.

Table 1
Statistics of data collection and processing.

Values in parentheses are for the highest resolution shell.

	A. suum QFR	*A. suum* QFR with flutolanil
X-ray source	BL44XU (SPring-8)	NW12A (Photon Factory)
Wavelength (Å)	0.900	1.000
Space group	$P2_12_12_1$	$P2_12_12_1$
Unit-cell parameters		
a (Å)	123.75	124.31
b (Å)	129.08	131.63
c (Å)	221.12	222.53
Resolution range (Å)	50.0–2.8 (2.9–2.8)	50.0–3.20 (3.35–3.20)
No. of reflections	587189	207156
Unique reflections	75372	54964
Completeness (%)	89.2 (58.8)	93.9 (84.1)
R_{merge}† (%)	10.5 (36.6)	11.5 (40.0)
$I/\sigma(I)$	8.4 (3.5)	17.4 (1.6)

† $R_{merge} = \sum_{hkl}\sum_i |I_i(hkl) - \langle I(hkl)\rangle| / \sum_{hkl}\sum_i I_i(hkl)$.

of SQR from pig heart mitochondria (Sun *et al.*, 2005; PDB code 1zoy). The sequence identities between the pig and *A. suum* enzymes are 70.4, 68.3, 34.8 and 46.3% for the Fp, Ip, CybL and CybS subunits, respectively. Using X-ray diffraction data in the resolution range 15.0–2.8 Å collected from the flutolanil-free QFR crystal, a promising solution with two molecules per asymmetric unit was obtained and an *R* factor of 0.45 was achieved when the model was subsequently subjected to rigid-body refinement. Starting from the molecular-replacement solution, the structures of the flutolanil-free and flutolanil-bound forms of the *A. suum* QFR are currently being refined and electron density corresponding to bound flutolanil has been identified. The structures of the *A. suum* QFR together with those of the QFRs from *Wolinella succinogenes* (Lancaster *et al.*, 1999) and *Escherichia coli* (Iverson *et al.*, 1999) and the SQRs from *E. coli* (Yankovskaya *et al.*, 2003), pig heart mitochondria (Sun *et al.*, 2005) and avian heart mitochondria (Huang *et al.*, 2006) should help to clarify the structure–function relationships in complex II. In addition, the structure of the *A. suum* QFR complexed with flutolanil should provide information for the structure-based design of anthelminthics.

We are grateful to the staff of BL44XU at SPring-8 and the staff of NW12 and BL-5A at Photon Factory for their help with the collection of X-ray diffraction data. This work was supported in part by a grant from the Japan Aerospace Exploration Agency and by Grants-in-Aid for Scientific Research on Priority Areas from the 21st Century COE Program (F-3), for Creative Scientific Research and Targeted Proteins Research Program from the Japanese Ministry of Education, Culture, Sports, Science and Technology (180 73004, 18GS0314 and 1903610), and for Scientific Research (B) from the Japan Society for the Promotion of Science (18370042). DKI was a research fellow supported by the Japan Society for the Promotion of Science.

References

Collaborative Computational Project, Number 4 (1994). *Acta Cryst.* D**50**, 760–763.
Ernster, L. & Nordenbrand, K. (1967). *Methods Enzymol.* **10**, 86–94.
Huang, L. S., Sun, G., Cobessi, D., Wang, A. C., Shen, J. T., Tung, E. Y., Anderson, V. E. & Berry, E. A. (2006). *J. Biol. Chem.* **281**, 5965–5972.
Inaoka, D. K., Sakamoto, K., Shimizu, H., Shiba, T., Kurisu, G., Nara, T., Aoki, T., Kita, K. & Harada, S. (2008). *Biochemistry*, **47**, 10881–10891.
Ito, Y., Muraguchi, H., Seshime, Y., Oita, S. & Yanagi, S. O. (2004). *Mol. Genet. Genomics*, **272**, 328–335.
Iverson, T. M., Luna-Chaves, C., Cecchini, G. & Rees, D. C. (1999). *Science*, **284**, 1961–1966.
Iwata, F., Shinjyo, N., Amino, H., Sakamoto, K., Islam, M. K., Tsuji, N. & Kita, K. (2008). *Parasitol. Int.* **57**, 54–61.
Jancarik, J. & Kim, S.-H. (1991). *J. Appl. Cryst.* **24**, 409–411.
Kita, K. & Takamiya, S. (2002). *Adv. Parasitol.* **51**, 95–131.
Lancaster, C. R. D., Kröger, A., Auer, M. & Michel, H. (1999). *Nature (London)*, **402**, 377–385.
Matsumoto, J., Sakamoto, K., Shinjyo, N., Kido, Y., Yamamoto, N., Yagi, K., Miyoshi, H., Nonaka, N., Katakura, K., Kita, K. & Oku, Y. (2008). *Antimicrob. Agents. Chemother.* **52**, 164–170.
Matthews, B. W. (1968). *J. Mol. Biol.* **33**, 491–497.
Miyadera, H., Shiomi, K., Ui, H., Yamaguchi, Y., Masuma, R., Tomoda, H., Miyoshi, H., Osanai, A., Kita, K. & Omura, S. (2003). *Proc. Natl Acad. Sci. USA*, **100**, 473–477.
Navaza, J. (1994). *Acta Cryst.* A**50**, 157–163.
Omura, S. *et al.* (2001). *Proc. Natl Acad. Sci. USA*, **98**, 60–62.
Otwinowski, Z. & Minor, W. (1997). *Methods Enzymol.* **276**, 307–326.
Sun, F., Huo, X., Zhai, Y., Wang, A., Xu, J., Su, D., Bartlam, M. & Rao, Z. (2005). *Cell*, **121**, 1043–1057.
Takamiya, S., Furushima, R. & Oya, H. (1984). *Mol. Biochem. Parasitol.* **13**, 121–134.
Tielens, A. G. M., Rotte, C., van Hellemond, J. J. & Martin, W. (2002). *Trends Biochem. Sci.* **27**, 564–572.
Yankovskaya, V., Horsefield, R., Törnroth, S., Luna-Chaves, C., Miyoshi, H., Léger, C., Byrne, B., Cecchini, C. & Iwata, S. (2003). *Science*, **299**, 700–704.

Mitochondrion 10 (2010) 158–165

Contents lists available at ScienceDirect

Mitochondrion

journal homepage: www.elsevier.com/locate/mito

Contribution of the FAD and quinone binding sites to the production of reactive oxygen species from *Ascaris suum* mitochondrial complex II

Madhavi P. Paranagama [a], Kimitoshi Sakamoto [a,*], Hisako Amino [a], Mutsumi Awano [a], Hideto Miyoshi [b], Kiyoshi Kita [a]

[a] Department of Biomedical Chemistry, Graduate School of Medicine, The University of Tokyo, 7-3-1 Hongo, Bunkyo-ku, Tokyo 113-0033, Japan
[b] Division of Applied Life Sciences, Graduate School of Agriculture, Kyoto University, Sakyo-ku, Kyoto 606-8502, Japan

ARTICLE INFO

Article history:
Received 1 May 2009
Received in revised form 22 October 2009
Accepted 9 December 2009
Available online 16 December 2009

Keywords:
Reactive oxygen species
Complex II
Ascaris suum

ABSTRACT

Reactive oxygen species (ROS) production from mitochondrial complex II (succinate–quinone reductase, SQR) has become a focus of research recently since it is implicated in carcinogenesis. To date, the FAD site is proposed as the ROS producing site in complex II, based on studies done on *Escherichia coli*, whereas the quinone binding site is proposed as the site of ROS production based on studies in *Saccharomyces cerevisiae*. Using the submitochondrial particles from the adult worms and L_3 larvae of the parasitic nematode *Ascaris suum*, we found that ROS are produced from more than one site in the mitochondrial complex II. Moreover, the succinate-dependent ROS production from the complex II of the *A. suum* adult worm was significantly higher than that from the complex II of the L_3 larvae. Considering the conservation of amino acids crucial for the SQR activity and the high levels of ROS production from the mitochondrial complex II of the *A. suum* adult worm together with the absence of complexes III and IV activities in its respiratory chain, it is a good model to examine the reactive oxygen species production from the mitochondrial complex II.

1. Introduction

The complex II superfamily comprises succinate–quinone reductase (SQR) and quinol-fumarate reductase (QFR), which catalyze the interconversion of succinate and fumarate with quinone and quinol. SQR is a component of the aerobic respiratory chain as well as the tricarboxylic acid cycle (for a review see Cecchini et al. (2002)). QFR is a component of the anaerobic respiratory chain in anaerobic and facultative anaerobic bacteria (Lancaster, 2004) and lower eukaryotes (Kita and Takamiya, 2002; Matsumoto et al., 2008; Van Hellmond et al., 2003).

SQR and QFR complexes generally consist of four subunits referred to as the flavoprotein subunit (Fp), iron-sulfur subunit (Ip), cytochrome *b* large subunit (CybL), and cytochrome *b* small subunit (CybS). The Fp and Ip subunits comprise the catalytic domain of the enzyme. The Fp subunit has an FAD as a prosthetic group and contains the dicarboxylate-binding site. The Ip subunit generally contains three iron-sulfur clusters $[2Fe–2S]^{2+,1+}$, $[4Fe–4S]^{2+,1+}$, and $[3Fe–4S]^{1+,0}$. Subunits CybL and CybS, with heme *b* as the prosthetic group, form the anchor domain of the enzyme. This anchors the catalytic domain to the inner mitochondrial membrane and also serves as the quinone oxidation/reduction site (for a review see Cecchini et al. (2002)).

Mutations in the Fp subunit in human complex II result in an infantile onset progressive neurodegenerative disease called Leigh syndrome (Ackrell, 2002; Bourgeron et al., 1995). Mutations in the Ip, CybL, and CybS subunits lead to cancers such as pheochromocytoma (tumours of the chromaffin cells in the adrenal medulla) and paraganglioma (extra adrenal tumours of sympathetic or parasympathetic origin) (Astuti et al., 2001; Bayley et al., 2006; Baysal et al., 2000; Baysal et al., 2002; Eng et al., 2003). Moreover, breast, thyroid, and renal carcinomas are associated with complex II mutations (Ni et al., 2008). However, the precise mechanism associating complex II mutations to carcinogenesis is not fully understood. Currently there are two hypotheses to explain how complex II mutations lead to carcinogenesis. One hypothesis suggests that succinate accumulation resulting from complex II dysfunction leads to stabilization of transcription factor hypoxia-inducible factor-1α (HIF-1α) by inhibiting HIF-1α prolyl hydroxylase (Briere et al., 2005; Cervera et al., 2008; Selak et al., 2005). The other hypothesis suggests that reactive oxygen species (ROS) generated from complex II defect result in oncogenesis (Guzy et al., 2008; Ishii et al., 2005). Thus, the mechanism of ROS generation from complex II has recently

Abbreviations: SQR, succinate:quinone reductase; QFR, quinol:fumarate reductase; SDH, succinate dehydrogenase; FRD, fumarate reductase; ROS, Reactive oxygen species; SOD, superoxide dismutase; SMP, submitochondrial particles.

* Corresponding author. Tel.: +81 3 5841 8202; fax: +81 3 5841 3444.
E-mail addresses: sakamok@m.u-tokyo.ac.jp, ndh1ascaris@yahoo.co.jp (K. Sakamoto).

1567-7249/$ - see front matter © 2009 Elsevier B.V. and Mitochondria Research Society. All rights reserved.
doi:10.1016/j.mito.2009.12.145

become a focus of research. Accumulating evidence indicates that ROS induce neoplasia by mutating nuclear and mitochondrial DNA (Ishii et al., 2005) or by signaling a pseudohypoxic condition by stabilization of the HIF-1α under normoxic conditions (Guzy et al., 2008). To date, the FAD site is proposed as the ROS producing site in complex II, based on studies done on *Escherichia coli* (Messner and Imlay, 2002), whereas the quinone binding site is proposed as the site of ROS production based on studies in *Saccharomyces cerevisiae* (Guo and Lemire, 2003; Szeto et al., 2007).

In adult worms of the parasitic helminth *Ascaris suum*, complex II functions as the terminal oxidase of the anaerobic respiratory chain and catalyzes fumarate reduction (quinol-fumarate reductase; QFR; Kita et al., 2007). Consistent with its physiological function, it shows high fumarate reductase (FRD) activity when the water-soluble dye methyl violegen is used as an artificial electron donor (Amino et al., 2003). Although the adult enzyme shows high FRD activity, the amino acid sequences of all four of its subunits are more similar to the mitochondrial SQR than to the bacterial QFR (Amino et al., 2000; Amino et al., 2003; Kuramochi et al., 1994; Saruta et al., 1995; Saruta et al., 1996). Moreover, the amino acid residues in the FAD binding site and the active site in the catalytic domain as well as the quinone binding site (Q site) are similar to the mitochondrial SQR. In addition, it shows high SQR activity *in vitro* (Iwata et al., 2008; Kita et al., 2002).

During a study of complex II in adult *A. suum*, we found a significant degree of succinate–cytochrome *c* reductase activity in purified *A. suum* adult complex II, even though the preparation did not contain complex III (quinol-cytochrome *c* reductase) (Takamiya et al., 1986). This result raised the possibility that significant electron leak occurred from adult complex II. In the present study, in attempting to verify this possibility, we investigated succinate-dependent ROS production from the parasite's mitochondria. Analysis of submitochondrial particles for superoxide (O_2^-) production using superoxide dismutase inhibitable acetylated cytochrome *c* reduction, and hydrogen peroxide production using catalase inhibitable amplex red oxidation, in the presence and absence of respiratory chain inhibitors, showed the contribution from both the FAD site and Q site of complex II to produce O_2^- and H_2O_2 when succinate is oxidized under aerobic conditions. Considering the conservation of amino acid residues critical for the enzyme reaction between *A. suum* complex II and mitochondrial SQR, our results show that ROS are produced from more than one site in mitochondrial complex II, linked with subtle differences in the amino acid sequences of the enzyme complex.

2. Materials and methods

2.1. Chemicals

Amplex red was obtained from Molecular probes (Eugene, Oregon). Acetylated cytochrome *c*, superoxide dismutase (bovine and *E. coli*), and horseradish peroxidase were from Sigma Chemical Company, USA. Catalase was from Wako, Japan. Atpenin A5 was from Alexis Biochemicals, Switzerland.

2.2. Submitochondrial particles (SMPs)

SMPs were prepared from frozen muscles of *A. suum* adult female worms by the modified method of Matsuno-Yagi and Hatefi (1985). During preparation of mitochondria, Chappell Perry buffer (100 mM KCl, 50 mM Tris–HCl, 1 mM ATP, 5 mM $MgCl_2$ and 1 mM EDTA, pH 7.4) containing 10 mM sodium malonate was used (Yamashita et al., 2004). Mitochondria were subjected to sonication four times for 30 s with 1.5-min intervals (Branson 450 D, Japan) in the same buffer containing 1 mM sodium malonate and $MgCl_2$ and $MnCl_2$ at a final concentration of 10 mM. In addition, the SMP were washed three times in Chappell Perry buffer with 1 mM sodium malonate buffer to remove the ROS scavenging molecules and stored at −80 °C. Mitochondria from L_3 larvae were prepared as previously described (Amino et al., 2003). SMPs were prepared from frozen mitochondria of *A. suum* L_3 larvae by sonicating three times for 30 s with 1.5-min intervals in a water bath sonifier (Sibata Su-25, Model SSC-350H, Japan). They were washed as described in adult SMP preparation and stored at −80 °C. The protein concentration in the SMP samples was estimated by Lowry's method (Lowry et al., 1951), using bovine serum albumin as the standard.

2.3. Superoxide generation assay

The superoxide radical generation rate was assayed using superoxide dismutase (SOD) inhibitable acetylated cytochrome *c* reduction (Azzi et al., 1975; Imlay and Fridovich, 1991; Zhao et al., 2006). The assay was performed in 50 mM potassium phosphate buffer (pH 7.4) containing, 0.25 M sucrose and 1 mM $MgCl_2$ at 25 °C in the presence of 25 μM acetyl cytochrome *c* and 15 μg/ml SMP in a total reaction mixture of 1 ml. After pre-incubating the mixture for 2 min, the reaction was started by adding 0.75 mM sodium succinate or 50 μM NADH. A parallel reaction was run with an additional 30 U/ml superoxide dismutase. The reduction of acetylated cytochrome *c* was monitored spectrophotometrically as the difference in absorbance at 550–540 nm and calculated using the difference in extinction coefficients of ferrocytochrome *c* and ferricytochrome *c*, $\varepsilon^{550-540} = 19\ mM^{-1}\ cm^{-1}$. Non-specific reduction of acetyl cytochrome *c* was excluded by subtracting the amount of cytochrome *c* reduced in the presence of SOD from that in the absence of SOD.

2.4. H_2O_2 generation assay

Oxidation of amplex red (10-acetyl-3,7-dihydroxyphenoxazine) to resorufin was used to assay the H_2O_2 generation rate (Chen et al., 2003; Mohanty et al., 1997; Shinjyo and Kita, 2007). The assay was performed in 50 mM potassium phosphate buffer (pH 7.4) containing, 0.25 M sucrose and 1 mM $MgCl_2$, 50 μmol amplex red, 0.2 U/ml horseradish peroxidase, 15 μg/ml SMP, and 0.75 mM sodium succinate or 50 μM NADH in a total reaction mixture of 1.0 ml maintained at 25 °C. A parallel reaction was run with an additional 1000 U/ml catalase. The resorufin formation rate was monitored spectrophotometrically at 571 nm. The H_2O_2 generation rate was calculated by using a standard curve. Specificity of the reaction was obtained by subtracting the amount of H_2O_2 produced in the presence of catalase from that in the absence of catalase.

In *A. suum* adult SMP, both the O_2^- and H_2O_2 generation assays were also performed in the presence of 10 mM sodium malonate which blocks the dicarboxylate-binding site of complex II; 400 nM atpenin A5, which blocks the Q site of complex II; and 40 nM quinazoline, which blocks the Q site of complex I. In *A. suum* L_3 larval SMP, 10 μM antimycin A (Qi site inhibitor of complex III), 5 μM stigmatellin (Qo site inhibitor of complex III), 5 μM rotenone (Q site inhibitor of complex I) were also employed in the assays. All these inhibitors at the above-mentioned concentrations reduced more than 85% of the corresponding activities.

2.5. Statistical analysis

All the assays were performed in triplicate and the results were expressed as means ± SEM. O_2^- or H_2O_2 production from a particular organism with a given substrate was compared between different experimental conditions using one-way analysis of

variance followed by the Tukey test. The level of significance was $p < 0.05$.

3. Results

3.1. Complex II is the main ROS producing site in the respiratory chain of adult A. suum

Since the presence of antioxidant molecules in the mitochondria interfered with accurate ROS detection, inside-out submitochondrial particles were prepared and washed to eliminate the antioxidant molecules. As shown in Figs. 1a and 1b, substantial production of O_2^- and H_2O_2 was observed from the submitochondrial particles of *A. suum* adults and L_3 larvae. Then, a series of respiratory chain inhibitors in combination with the respiratory substrates were employed in the assays in order to localize the site of ROS production. Quinazoline is a Q site inhibitor of *A. suum* adult complex I (Yamashita et al., 2004) (Fig. 2a). During succinate oxidation, i.e., electron entry into the respiratory chain from complex II, the addition of quinazoline inhibits the reverse flow of electrons into complex I from the quinone pool. As shown in Table 1, quinazoline inhibition did not show a significant effect on succinate-dependent O_2^- production. This result indicates that the contribution of complex I for succinate-dependent ROS production in *A. suum* adult worms is not significant. Since complex III and IV activities are not found in the respiratory chain of adult *A. suum*, the only significant source of O_2^- in its submitochondrial particles must be complex II. Moreover, the addition of quinazoline in the reaction mixture during NADH oxidation, i.e., electron entry from complex I, resulted in 95% suppression of the O_2^- production rate (Table 1) suggesting the possibility of either the Q site of complex I or a redox center/centers in complex II to be the major O_2^- production sites. In order to assess the contribution of the Q site in complex I for O_2^- production, atpenin A5, which inhibits the SQR activity of complex II completely in *A. suum* (Miyadera et al., 2003) (Fig. 2a), was employed. The NADH-dependent O_2^- production rate observed in the presence of atpenin A5 was not significantly different from that in the presence of quinazoline (Table 1), indicating that the Q site of complex I does not contribute to NADH-dependent O_2^- production significantly. The effect of inhibitors on succinate- and NADH-dependent hydrogen peroxide production rates also showed a similar pattern to that of O_2^- (data not shown). Collectively, the above data provide clear evidence to show that complex II is the main ROS producing site in the respiratory chain of *A. suum* adult worms.

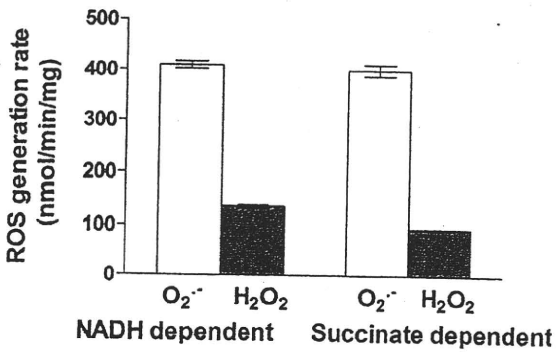

Fig. 1a. Superoxide and hydrogen peroxide generation by SMP of adult *A. suum* worms oxidizing 0.75 mM succinate or 50 μM NADH. Superoxide production was measured as superoxide dismutase inhibitable reduction of acetylated cytochrome c, and hydrogen peroxide production was measured as catalase inhibitable oxidation of amplex red as described in Section 2. Results are expressed as means ± SEM of triplicate measurements from three different pools of submitochondrial particles.

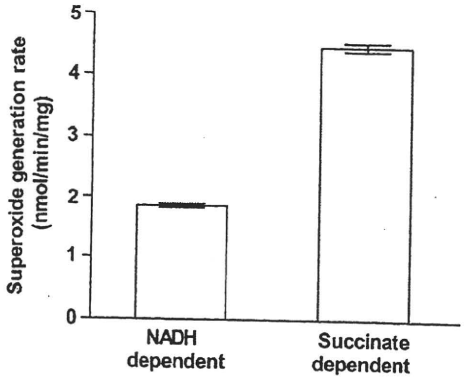

Fig. 1b. Superoxide generation by SMP of *A. suum* L_3 larvae oxidizing 0.5 mM succinate or 50 μM NADH. Superoxide production was measured as superoxide dismutase inhibitable reduction of acetylated cytochrome c as described in Section 2. Results are expressed as means ± SEM of triplicate measurements from a single pool of submitochondrial particles. No detectable level of hydrogen peroxide was produced when measured as catalase inhibitable oxidation of amplex red as described in Section 2.

Table 1
Superoxide production from submitochondrial particles of *A. suum* adult worms oxidizing 0.5 mM succinate and 50 μM NADH in the presence of respiratory chain inhibitors. Superoxide production was determined as superoxide dismutase inhibitable reduction of acetylated cytochrome c as described in Secton 2. Values are given as nmol/min/mg of protein and expressed as means ± SEM from triplicate measurements on one pool of submitochondrial particles. The decrease of superoxide production (%) in the presence of the inhibitor compared to that in the absence of the inhibitor is given in parentheses.

	Succinate	NADH
No inhibitor	400 ± 11	410 ± 7.75
Quinazoline (40 nM)	359 ± 12 (−10%)	21.1 ± 1.01[b] (−95%)
Atpenin A5 (400 nM)	246 ± 5[a] (−38%)	24.0 ± 0.58[b] (−94%)
Malonate (10 mM)	ND[d]	67.8 ± 4.21[c] (−83%)

[a,b,c] Significantly different from the measurement without an inhibitor. $p < 0.05$.
There was no significant difference between [b]$p < 0.05$.
There was a significant difference between [b]and [c]$p < 0.05$.
[d] ND: not detectable.

3.2. ROS production from the respiratory chain of A. suum L_3 larvae

In *A. suum* L_3 larvae, components of the respiratory chain are similar to those of mammalian mitochondria (Kita and Takamiya, 2002), and complex II serves as SQR. Since the subunit composition of L_3 larvae complex II is different from that of the adult worm (Amino et al., 2000; Amino et al., 2003), succinate- and NADH-dependent ROS production from the SMP of L_3 larvae was also measured in the presence of 5 μM rotenone (Q site inhibitor of complex I), 10 μM antimycin A (Qi site inhibitor of complex III), 5 μM stigmatellin (Qo site inhibitor of complex III), and 10 mM NaN_3 (complex IV inhibitor). In L_3 larvae, the succinate-dependent O_2^- production rate was not significantly affected by the addition of these inhibitors (Table 2). This suggests that complexes I, III, and IV of the L_3 larval respiratory chain do not contribute to O_2^- production during succinate oxidation. Yet, O_2^- production during succinate oxidation was almost completely inhibited by 10 mM malonate and 14% inhibited by atpenin A5. Taken together, these data indicate that complex II is the main succinate-dependent ROS producing site in the submitochondrial particles of *A. suum* L_3 larvae, as is the case for adult worms. On the other hand, malonate and atpenin A5 did not have any effect on NADH-dependent O_2^- production, whereas rotenone significantly increased it. O_2^- production rates in the presence of antimycin A and stigmatellin or NaN_3 were similar to that in the presence of rotenone. These

Table 2
Superoxide production from submitochondrial particles of *A. suum* L_3 larvae oxidizing 0.5 mM succinate or 50 μM NADH in the presence of respiratory chain inhibitors. Superoxide production was determined as superoxide dismutase inhibitable reduction of acetylated cytochrome *c* as described in Section 2. Values are given as nmol/min/mg of protein expressed as means ± SEM from triplicate measurements on one pool of submitochondrial particles. The change of superoxide production (%) in the presence of the inhibitor compared to that in the absence of the inhibitor is given in parentheses.

	Succinate	NADH
No inhibitor	4.45 ± 0.07	1.86 ± 0.03
Rotenone (5 μM)	4.42 ± 0.03 (−0.7%)	2.29 ± 0.07[b] (+23%)
Antimycin A (10 μM)	4.56 ± 0.07 (+3%)	1.62 ± 0.07 (−13%)
Antimycin A (10 μM) + Stigmatellin (5 μM)	4.81 ± 0.03 (+8%)	2.53 ± 0.03[b] (+36%)
NaN_3 (10 mM)	4.87 ± 0 (+9%)	2.63 ± 0.04[b] (+41%)
Malonate (10 mM)	ND[d]	1.62 ± 0.13 (−13%)
Atpenin A5 (400 nM)	3.85 ± 0.07[a] (−14%)	1.82 ± 0.01 (−2%)

[a,b] Significantly different from the measurement without an inhibitor. $p < 0.05$. There was no significant difference among [b] $p < 0.05$.
[d] ND: not detectable.

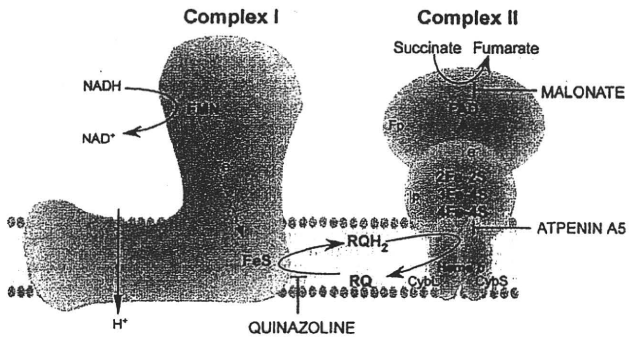

Fig. 2a. Schematic representation of the flow of electrons and the sites of action of inhibitors in the respiratory chain complexes of *A. suum* adult worms.

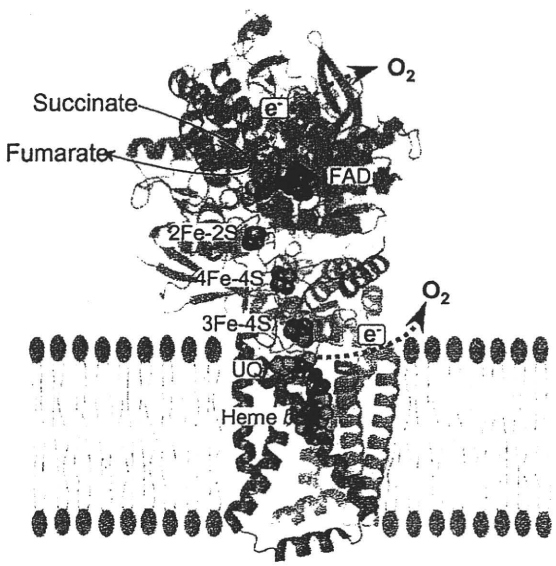

Fig. 2b. Ribbon model of mitochondrial complex II of *S. scrofa* (pdb1ZOY) showing the potential reactive oxygen species production sites identified in *A. suum*. Fp, Ip, CybL and CybS subunits are shown in green, blue, red and orange respectively. The redox centers, FAD, iron-sulfur clusters and heme *b* are as labeled in the figure. Rhodoquinone is supposed to bind to the position of ubiquinone.

observations imply that a redox center in complex I upstream to its Q site is the source of NADH-dependent O_2^- in L_3 larvae. Blocking of complexes III or IV leads to accumulation of electrons at complex I, enhancing the O_2^- production from this site in a similar manner to rotenone. Interestingly, unlike in many mammalian tissues, blocking of the Qi site in complex III did not increase the O_2^- production by submitochondrial particles of L_3 larvae. A quantitative comparison of ROS production between complexes I and II in *A. suum* L_3 larvae showed that the succinate-dependent O_2^- production from complex II is 3-fold higher than NADH-dependent O_2^- production from complex I (Table 2).

3.3. ROS are produced from more than one site in A. suum mitochondrial complex II

In *E. coli*, the flavin of complex IIs is considered to be the source of ROS (Messner and Imlay, 2002). In these enzymes, succinate-dependent ROS production is at a maximum at a lower succinate concentration (at about 1 mM), and at higher succinate concentrations (around 50–100 mM), it is completely inhibited. Hence, excess succinate is suggested to suppress ROS production by hindering the access of oxygen to FAD, thus preventing its autoxidation. When we measured the succinate-dependent ROS production in *A. suum* SMP, it increased with substrate concentration and was highest at 0.5–1 mM succinate in both adults and L_3 larvae (Fig. 3) and gradually decreased along with increasing succinate concentrations. This finding is in accordance with the findings on *E. coli* complex IIs by Messner and Imlay (2002).

However, the percentage of inhibition in ROS production at ⩾100 mM succinate in *A. suum* complex II was only 80%, with 20% always remaining. Further, as shown in Table 1, NADH-dependent O_2^- production was only 83% suppressed by the addition of 10 mM malonate into the reaction mixture. Since malonate is a succinate analogue, which is also known to bind in close proximity to the FAD site in mitochondrial complex II (Huang et al., 2006), it is likely to block the interaction between *A. suum* FAD and oxygen in a manner similar to that in *E. coli* complex IIs, thus decreasing the O_2^- production from the FAD site. Such residual ROS production observed even after complete blocking of the FAD site with succinate or malonate suggests another site for ROS production, in addition to FAD.

The Q site is the other candidate for a potential source of ROS in complex II as reported by Guo and Lemire (2003), and Zhao et al.,

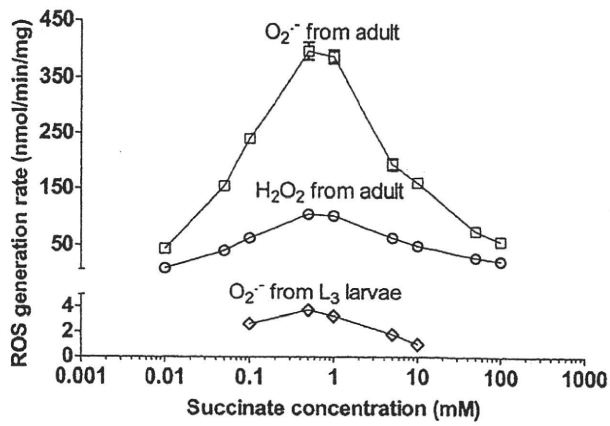

Fig. 3. Effect of succinate concentration on ROS production from *A. suum* SMP. Reaction media for superoxide and hydrogen peroxide measurements were prepared as described in Section 2. Reactions were initiated by addition of succinate at a concentration range of 0.01–100 mM. Points indicate means ± SEM in triplicate measurements from three different pools of SMPs in adult worms and from a single pool in L_3 larvae.

2006. To determine the contribution of the Q site of *A. suum* complex II to ROS production, we analyzed its ROS production in the presence of 400 nM atpenin A5, which inhibits the Q site of complex II completely. O_2^- production from complex II of *A. suum* adult worms with 0.75 mM succinate was decreased 38% in the presence of atpenin A5 (Table 1). In L_3 larvae, it was decreased approximately 14% (Table 2). This observation indicates that binding of atpenin A5 results in reduction in ROS production from *A. suum* complex IIs. In another ROS producing system, xanthine oxidase/hypoxanthine, atpenin A5 interfered with neither ROS production nor detection (data not shown), suggesting that atpenin A5 does not serve as a radical scavenger. Thus, it appears that electrons leak to oxygen from the Q site also during succinate oxidation. Atpenin A5 may inhibit either binding and/or reduction of quinone, thus preventing electron flow in the Q site and inhibiting ROS production.

4. Discussion

Mitochondrial respiratory chain is a significant source of cellular ROS. Impairment of the respiratory chain complexes is known to increase the cellular ROS production (Indo et al., 2007). Historically, complexes I and III are considered as the two major sites of superoxide and hydrogen peroxide production in the respiratory chain (Jezek and Hlavata, 2005; Murphy, 2009; St-Pierre et al., 2002). Interestingly, our results show that complex II is the main site of ROS production in *A. suum* adult respiratory chain (Table 1). In *A. suum* adult respiratory chain, complex II produces equally high amount of superoxide and hydrogen peroxide during the oxidation of the complex I linked substrate NADH and the complex II linked substrate succinate, even under uninhibited conditions (Table 1). This observation is contradictory to the observations so far reported for the mitochondrial respiratory chain in other organisms. Generally, the respiratory chain of isolated mammalian and avian mitochondria and submitochondrial particles respiring under uninhibited conditions produce significant amount of ROS only during succinate oxidation by complex II, but the site of ROS production is not intrinsic to complex II. In this situation, ROS are produced from complex I during the reversed flow of electrons derived from succinate oxidation to reduce NAD (Liu et al., 2002). It is completely abolished by rotenone which inhibits the Q site of complex I (Liu et al., 2002; Muller et al., 2008). One can argue that electrons originating from succinate oxidation in the mitochondrial complex II of *A. suum* adult worm also may flow in the reverse direction through the complex I and leak to oxygen, due to the absence of complexes III and IV activities in its respiratory chain. However, reversed flow of electrons through complex I was not found to be a significant mode of ROS production in the *A. suum* adult respiratory chain since inhibition of the Q site in complex I with quinazoline inhibited only 10% of the succinate-dependent ROS production (Table 1). Another feature of the *A. suum* adult respiratory chain is that it produces significantly high amount of ROS even when the succinate concentration is as low as 10 μM (Fig 3). At such lower concentrations of succinate, detectable level of ROS production is not so far reported from the mitochondrial respiratory chain in other organisms. Similar to our findings, succinate-dependent ROS production intrinsic to complex II was reported from the mitochondrial respiratory chain in *S. cerevisiae* (Guo and Lemire, 2003; Szeto et al., 2007) and *C. elegans* (Senoo-Matsuda et al., 2001; Huang and Lemire, 2009), but the amounts of ROS produced by their complex II were significantly lower than that from *A. suum* adult complex II reported in this study.

It is well established that ROS production is negligible during the oxidation of NADH linked substrates by the uninhibited mitochondrial respiratory chain, but inhibition of the Q site of complex I with an inhibitor such as rotenone results in NADH-dependent ROS production from complex I to a significant level (Hirst et al., 2008). In contrast, addition of the complex I inhibitor quinazoline or the complex II Q site inhibitor aptenin A5 during NADH oxidation in *A. suum* adult SMP almost completely abolished the ROS production detected under uninhibited conditions (Table 1), indicating that complex II is the principal ROS producing site even during NADH oxidation. Thus, our present study shows that *A. suum* adult complex II has the unique feature of significantly high amounts of intrinsic ROS production during oxidation of both the complex I and II linked substrates under uninhibited conditions.

Although it is widely accepted that complex II of the mitochondrial respiratory chain does not have an intrinsic ROS generation under physiological conditions, accumulating evidence indicates that pathogenic mutations in complex II can result in electron leak to oxygen and produce ROS. Simulation of these pathogenic mutations by pharmacological inhibition of complex II activity with thionyl trifluoroacetate (TTFA) (Eto et al., 1992; Guzy et al., 2008) and by genetic inhibition of complex II activity by RNA interference of the Ip subunit (Guzy et al., 2008) has been reported to induce succinate-dependant ROS production, probably due to formation of a flavin radical in the Fp subunit of complex II. In addition, purified and solubilized mitochondrial complex II is also shown to produce ROS through a similar manner (Zhang et al., 1998). Moreover, it has been postulated that ROS may be produced from complex II, if the enzyme is damaged by oxidative stress or ageing also (Jezek and Hlavata, 2005).

Understanding the ROS producing sites in complex II is important in addressing complex II associated diseases linked with ROS production. Currently, there are two models regarding the ROS production site in respiratory chain complex II. One model is based on studies carried out on *E. coli* complex IIs and postulates that the FAD site in the Fp subunit is the principal site of ROS production (Messner and Imlay, 2002; Yankovskaya et al., 2003). Exposure of FAD to the aqueous environment and high electron density are identified as the causes for ROS production from FAD site. This condition is a consequence of interference in electron flow through other redox centers. The other model, based on studies carried out in *S. cerevisiae*, postulates that the ubiquinone-binding site is the major ROS production site. Mutations in Ip, CybL, and CybS subunits are suggested to alter the ubiquinone-binding site, resulting in electron leak (Guo and Lemire, 2003; Szeto et al., 2007).

To gain further insight into ROS production from complex II, we used complex II of the *A. suum* adult worm since it has a high sequence similarity to mitochondrial SQR and produces a significantly high amount of ROS (Fig. 1a). As shown in Table 1, when succinate is utilized as the respiratory substrate, complete inhibition of the Q site of *A. suum* adult respiratory chain with atpenin A5 diminished the level of ROS production by 38%. Since complexes III and IV activities are not detected in *A. suum* adult respiratory chain and the contribution of complex I for succinate-dependent ROS production is not significant (Table 1), this result indicates the possibility of the Q site of the complex II in succinate-dependent ROS generation. The remaining fraction (62%) of the succinate-dependent ROS are likely to be originated from the redox centers located between the Q binding site and the succinate oxidation site in complex II. Those are the Fe-S clusters in the Ip subunit and the FAD site in the Fp subunit. Since Fe-S clusters are buried below the solvent accessible surface of the protein molecule while FAD is localized exposed to the aqueous environment (Sun et al., 2005; Yankovskaya et al., 2003), the probable contributor for the remaining fraction of the ROS appears to be the FAD site. As we have discussed in Section 3.3, the strong suppression of succinate-dependent ROS production at high concentrations of succinate provide evidence for the involvement of FAD site in succinate-dependent ROS production in *A. suum* mitochondrial

complex II. Thus, our data are in accordance with both models of ROS production from complex II (Fig. 2b).

4.1. ROS production from the FAD site

The only other complex II that is so far reported to produce such a high level of ROS from the FAD site is *E. coli* QFR. However, the Fp subunit of *A. suum* adult complex II (QFR) displayed only 37% sequence identity to that of *E. coli* QFR whereas its sequence identity to that of human Fp is much higher (68%). Moreover, the amino acid residues participating in the FAD and dicarboxylate-binding sites in *A. suum* adult complex II are identical to those in the mitochondrial SQR, but not to those in *E. coli* QFR. These observations indicate that the roles of the amino acid residues involved in interacting with FAD and substrate binding in QFR of *E. coli* and *A. suum* are different, although they share in common a high level of FRD activity and ROS production. In contrast, the SQR of *E. coli* has a low level of ROS production (Messner and Imlay, 2002). We also observed a low level of ROS production from complex II in *A. suum* L_3 larvae (Fig. 1b), which has low FRD/SQR activity (0.39) (Amino et al., 2003) despite its high sequence similarity to that of its adult counterpart.

As shown for *E. coli* complex IIs, the principal difference between SQR and QFR lies in the arrangement of redox potentials among the redox centers (Yankovskaya et al., 2003). In *E. coli* QFR, FAD and the 2Fe–2S cluster have the highest redox potentials, thus attracting electrons to fumarate. On the other hand, in *E. coli* SQR, heme *b* and 3Fe–4S have the highest redox potentials, attracting electrons to quinone. These redox potentials are known to be important to drive the electrons in the direction of the physiological reaction of the respective enzymes. Succinate oxidation in SQR and quinol oxidation in QFR leads the enzymes to a reduced state with two electrons. According to theoretical calculations, the distribution of electrons around FAD in the reduced enzyme is 50 times greater in QFR compared to that in SQR in *E. coli* (Yankovskaya et al., 2003). This provides further evidence to the proposal by Messner and Imlay (2002) that the reduced state around FAD is the cause of the high level of ROS production by *E. coli* QFR. Since complex II of *A. suum* adult worms also shows high fumarate reductase activity, it is reasonable to speculate that electrons will sequestrate on its FAD during succinate oxidation with subsequent leak to oxygen.

It appears that, despite the remarkable identity in the amino acid residues interacting with FAD and forming the substrate binding site of *A. suum* adult complex II and mitochondrial SQR, sequestration of electrons on FAD and subsequent leak to oxygen are the features mainly connected to the ability to reduce fumarate by *A. suum* adult complex II. Based on these observations, it is likely that some mutations in mitochondrial SQR may result in accumulation of electrons on FAD and subsequent leakage to oxygen. In fact, it has been shown that mitochondrial complex II produces ROS in pulmonary vasculature due to the reverse flow of electrons under hypoxic conditions (Paddenberg et al., 2003).

4.2. ROS production from the quinone binding site

As shown in Tables 1 and 2, succinate-dependent ROS production from *A. suum* SMP is considerably diminished when the complex II Q site is inhibited with atpenin A5, indicating that the quinone binding site also is a contributor for ROS production from *A. suum* complex II. The quinone binding site is formed by amino acid residues which reside in Ip, CybL, and CybS subunits. Generally, it leaks electrons to oxygen either via a destabilized quinone molecule or directly from the site. To reduce the quinone in complex II completely, two electrons are needed. However, electrons are transferred one at a time from the 3Fe–4S center to the quinone bound at the Q site. Thus, a semiquinone intermediate is an obligatory part of the quinone reduction by complex II. Until another electron arrives, the protein environment of the Q-site donates a proton and stabilizes the semiquinone, thereby preventing its release from the Q site or premature reoxidation. In the latter case, a reduction in the affinity of the Q site for quinone can result in direct transfer of electrons to oxygen from the Q site (Horsefield et al., 2006; Szeto et al., 2007).

As shown by Lemire and colleagues, using the SQR of *S. cerevisiae*, mutations in the amino acid residues associated with quinone binding and reduction lead to high levels of ROS production from the Q site (Guo and Lemire, 2003; Szeto et al., 2007). Yet, except for replacement of Ile C28 with Gly, the amino acid residues important for quinone binding and reduction in SQR enzymes are conserved in *A. suum* adult complex II. Thus, the replacement of Ile C28 to Gly seems to be responsible for ROS production, but this idea is not supported by the sequence of free-living nematode *C. elegans*, which also has Gly in that position without producing significant amounts of ROS. In addition, complex II in *S. cerevisiae*, which has Ser instead of Ile in the corresponding position, also is reported to produce very low amounts of ROS (Guo and Lemire, 2003).

When the conservation of amino acid residues responsible for quinone binding and reduction between mitochondrial SQR and *A. suum* adult complex II, which functions as QFR, are considered together with the high level of ROS production observed only from *A. suum* adult complex II, it appears that differences in the architecture of the quinone binding site caused by subtle differences in its amino acid residues may contribute to the high level of ROS production from its Q site. These differences may result in either an increase in the flow of electrons out of the enzyme or the formation of a destabilized semiquinone radical during quinone reduction, leading to a high degree of ROS production. However, we cannot rule out the possibility of the contribution of rhodoquinone for ROS production from its Q site. Rhodoquinone, which has a lower redox potential (−63 mV) compared to ubiquinone (+110 mV), is a more favorable electron donor to oxygen than ubiquinone (Kita and Takamiya, 2002). In this regard, it is also noteworthy that the Q site in *E. coli* QFR is not known to produce ROS (Messner and Imlay, 2002) despite the presence of menaquinone, which has an even lower redox potential than that of rhodoquinone (−80 mV) (Cecchini et al., 2002). Thus, the presence of a low potential quinone does not appear to be a likely cause of the high level of ROS production from the Q site in *A. suum* adult complex II.

5. Conclusion

We have shown here that under aerobic conditions, both the FAD site and quinone binding site in *A. suum* adult complex II contribute to produce significantly high amounts of O_2^- and H_2O_2 during succinate oxidation, despite its high sequence similarity to mammalian SQR, which does not produce ROS. According to our observations, subtle amino acid differences in complex II subunits may result in leakage of electrons originating from succinate oxidation from more than one site in complex II, forming ROS. Since the amino acids interacting with FAD and participating in succinate binding and quinone reduction in *A. suum* complex II are well conserved, amino acid residues responsible for high reactivity with oxygen may be localized in unique sequences in the parasite's enzyme complex.

In summary, this study shows significant release of ROS from the mitochondrial complex II using the unique *A. suum* model. We believe that *A. suum* adult complex II is a good model to study the mechanism of ROS production from mitochondrial complex II, since amino acid residues conserved among the catalytic domains

in mitochondrial SQR enzymes are well conserved in this enzyme and it produces high levels of ROS. Absence of complex III and IV activities in its respiratory chain is an additional advantage of this model. Analysis of its crystal structure and expression of its subunits in a cell-free system for mutational analysis are in progress. These studies will provide further insight into the possibility of high levels of ROS production from both the FAD site and the Q site in the complex II of *A. suum* adult worm and help to understand the role of mutations in human complex II for carcinogenesis.

Acknowledgements

This work was supported by a grant-in-aid for scientific research on Priority Areas (18073004), Creative Scientific Research (18GS0314), and Targeted Proteins Research Program to KK and by a Japanese Government scholarship to MPP from the Japanese Ministry of Education, Science, Culture, Sports and Technology.

References

Ackrell, B.A., 2002. Cytopathies involving mitochondrial complex II. Mol. Aspects. Med. 23, 369–384.

Amino, H., Osanai, A., Miyadera, H., Shinjyo, N., Tomitsuka, E., Taka, H., Mineki, R., Murayama, K., Takamiya, S., Aoki, T., Miyoshi, H., Sakamoto, K., Kojima, S., Kita, K., 2003. Isolation and characterization of the stage-specific cytochrome b small subunit (CybS) of *Ascaris suum* complex II from the aerobic respiratory chain of larval mitochondria. Mol. Biochem. Parasitol. 128, 175–186.

Amino, H., Wang, H., Hirawake, H., Saruta, F., Mizuchi, D., Mineki, R., Shindo, N., Murayama, K., Takamiya, S., Aoki, T., Kojima, S., Kita, K., 2000. Stage-specific isoforms of *Ascaris suum* complex. II: The fumarate reductase of the parasitic adult and the succinate dehydrogenase of free-living larvae share a common iron–sulfur subunit. Mol. Biochem. Parasitol. 106, 63–76.

Astuti, D., Latif, F., Dallol, A., Dahia, P.L., Douglas, F., George, E., Skoldberg, F., Husebye, E.S., Eng, C., Maher, E.R., 2001. Gene mutations in the succinate dehydrogenase subunit SDHB cause susceptibility to familial pheochromocytoma and to familial paraganglioma. Am. J. Hum. Genet. 69, 49–54.

Azzi, A., Montecucco, C., Richter, C., 1975. The use of acetylated ferricytochrome c for the detection of superoxide radicals produced in biological membranes. Biochem. Biophys. Res. Commun. 65, 597–603.

Bayley, J.P., van Minderhout, I., Weiss, M.M., Jansen, J.C., Oomen, P.H., Menko, F.H., Pasini, B., Ferrando, B., Wong, N., Alpert, L.C., Williams, R., Blair, E., Devilee, P., Taschner, P.E., 2006. Mutation analysis of SDHB and SDHC: novel germline mutations in sporadic head and neck paraganglioma and familial paraganglioma and/or pheochromocytoma. BMC Med. Genet. doi:10-1186/1471-2350-7-1.

Baysal, B.E., Ferrell, R.E., Willett-Brozick, J.E., Lawrence, E.C., Myssiorek, D., Bosch, A., van der Mey, A., Taschner, P.E., Rubinstein, W.S., Myers, E.N., Richard 3rd, C.W., Cornelisse, C.J., Devilee, P., Devlin, B., 2000. Mutations in SDHD, a mitochondrial complex II gene, in hereditary paraganglioma. Science 287, 848–851.

Baysal, B.E., Willett-Brozick, J.E., Lawrence, E.C., Drovdlic, C.M., Savul, S.A., McLeod, D.R., Yee, H.A., Brackmann, D.E., Slattery 3rd, W.H., Myers, E.N., Ferrell, R.E., Rubinstein, W.S., 2002. Prevalence of SDHB, SDHC, and SDHD germline mutations in clinic patients with head and neck paragangliomas. J. Med. Genet. 39, 178–183.

Bourgeron, T., Rustin, P., Chretien, D., Birch-Machin, M., Bourgeois, M., Viegas-Pequignot, E., Munnich, A., Rotig, A., 1995. Mutation of a nuclear succinate dehydrogenase gene results in mitochondrial respiratory chain deficiency. Nat. Genet. 11, 144–149.

Briere, J.J., Favier, J., Benit, P., El Ghouzzi, V., Lorenzato, A., Rabier, D., Di Renzo, M.F., Gimenez-Roqueplo, A.P., Rustin, P., 2005. Mitochondrial succinate is instrumental for HIF1alpha nuclear translocation in SDHA-mutant fibroblasts under normoxic conditions. Hum. Mol. Genet. 14, 3263–3269.

Cecchini, G., Schroder, I., Gunsalus, R.P., Maklashina, E., 2002. Succinate dehydrogenase and fumarate reductase from *Escherichia coli*. Biochim. Biophys. Acta. 1553, 140–157.

Cervera, A.M., Apostolova, N., Crespo, F.L., Mata, M., McCreath, K.J., 2008. Cells silenced for SDHB expression display characteristic features of the tumor phenotype. Cancer Res. 68, 4058–4067.

Chen, Q., Vazquez, E.J., Moghaddas, S., Hoppel, C.L., Lesnefsky, E.J., 2003. Production of reactive oxygen species by mitochondria: central role of complex III. J. Biol. Chem. 278, 36027–36031.

Eng, C., Kiuru, M., Fernandez, M.J., Aaltonen, L.A., 2003. A role for mitochondrial enzymes in inherited neoplasia and beyond. Nat. Rev. Cancer 3, 193–202.

Eto, Y., Kang, D., Hasegawa, E., Takeshige, K., Minakami, S., 1992. Succinate-dependent lipid peroxidation and its prevention by reduced ubiquinone in beef heart submitochondrial particles. Arch. Biochem. Biophys. 295, 101–106.

Guo, J., Lemire, B.D., 2003. The ubiquinone-binding site of the *Saccharomyces cerevisiae* succinate–ubiquinone oxidoreductase is a source of superoxide. J. Biol. Chem. 278, 47629–47635.

Guzy, R.D., Sharma, B., Bell, E., Chandel, N.S., Schumacker, P.T., 2008. Loss of the SdhB, but Not the SdhA, subunit of complex II triggers reactive oxygen species-dependent hypoxia-inducible factor activation and tumorigenesis. Mol. Cell Biol. 28, 718–731.

Hirst, J., King, M.S., Pryde, K.R., 2008. The production of reactive oxygen species by complex I. Biochem. Soc. Trans. 36, 976–980.

Horsefield, R., Yankovskaya, V., Sexton, G., Whittingham, W., Shiomi, K., Omura, S., Byrne, B., Cecchini, G., Iwata, S., 2006. Structural and computational analysis of the quinone-binding site of complex II (succinate–ubiquinone oxidoreductase): a mechanism of electron transfer and proton conduction during ubiquinone reduction. J. Biol. Chem. 281, 7309–7316.

Huang, J., Lemire, B.D., 2009. Mutations in the *C. elegans* succinate dehydrogenase iron-sulfur subunit promote superoxide generation and premature aging. J. Mol. Biol. 387, 559–569.

Huang, L.S., Shen, J.T., Wang, A.C., Berry, E.A., 2006. Crystallographic studies of the binding of ligands to the dicarboxylate site of Complex II, and the identity of the ligand in the "oxaloacetate-inhibited" state. Biochim. Biophys. Acta 1757, 1073–1083.

Imlay, J.A., Fridovich, I., 1991. Assay of metabolic superoxide production in *Escherichia coli*. J. Biol. Chem. 266, 6957–6965.

Indo, H.P., Davidson, M., Yen, H.C., Suenaga, S., Tomita, K., Nishii, T., Higuchi, M., Koga, Y., Ozawa, T., Majima, H.J., 2007. Evidence of ROS generation by mitochondria in cells with impaired electron transport chain and mitochondrial DNA damage. Mitochondrion 7, 106–118.

Ishii, T., Sakurai, T., Usami, H., Uchida, K., 2005. Oxidative modification of proteasome: identification of an oxidation-sensitive subunit in 26S proteasome. Biochemistry 44, 13893–13901.

Iwata, F., Shinjyo, N., Amino, H., Sakamoto, K., Islam, M.K., Tsuji, N., Kita, K., 2008. Change of subunit composition of mitochondrial complex II (succinate–ubiquinone reductase/quinol-fumarate reductase) in *Ascaris suum* during the migration in the experimental host. Parasitol. Int. 57, 54–61.

Jezek, P., Hlavata, L., 2005. Mitochondria in homeostasis of reactive oxygen species in cell, tissues, and organism. Int. J. Biochem. Cell Biol. 37, 2478–2503.

Kita, K., Hirawake, H., Miyadera, H., Amino, H., Takeo, S., 2002. Role of complex II in anaerobic respiration of the parasite mitochondria from *Ascaris suum* and *Plasmodium falciparum*. Biochim. Biophys. Acta 1553, 123–139.

Kita, K., Takamiya, S., 2002. Electron-transfer complexes in Ascaris mitochondria. Adv. Parasitol. 51, 95–131.

Kita, K., Shiomi, K., Ōmura, S., 2007. Parasitology in Japan: advances in drug discovery and biochemical studies. Trends. Parasitol. 23, 223–229.

Kuramochi, T., Hirawake, H., Kojima, S., Takamiya, S., Furushima, R., Aoki, T., Komuniecki, R., Kita, K., 1994. Sequence comparison between the flavoprotein subunit of the fumarate reductase (complex II) of the anaerobic parasitic nematode, *Ascaris suum* and the succinate dehydrogenase of the aerobic, free-living nematode, *Caenorhabditis elegans*. Mol. Biochem. Parasitol. 68, 177–187.

Lancaster, C.R.D., 2004. Structure and function of succinate: quinone oxidoreductases and the role of quinol: fumarate reductases in fumarate respiration. In: Zannoni, D. (Ed.), Respiration in Archaea and Bacteria: Diversity of Prokaryotic Electron Transport Carriers. Kluwer Academic Publishers, The Netherlands, pp. 57–85.

Liu, Y., Fiskum, G., Schubert, D., 2002. Generation of reactive oxygen species by the mitochondrial electron transport chain. J. Neurochem. 80, 780–787.

Lowry, O.H., Rosebrough, N.J., Farr, A.L., Randall, R.J., 1951. Protein measurement with the Folin phenol reagent. J. Biol. Chem. 193, 265–275.

Matsumoto, J., Sakamoto, K., Shinjyo, N., Kido, Y., Yamamoto, N., Yagi, K., Miyoshi, H., Nonaka, N., Katakura, K., Kita, K., Oku, Y., 2008. Anaerobic NADH-fumarate reductase system is predominant in the respiratory chain of *Echinococcus multilocularis*, providing a novel target for the chemotherapy of alveolar echinococcosis. Antimicrob. Agents Chemother. 52, 164–170.

Matsuno-Yagi, A., Hatefi, Y., 1985. Studies on the mechanism of oxidative phosphorylation. Catalytic site cooperativity in ATP synthesis. J. Biol. Chem. 260, 11424–11427.

Messner, K.R., Imlay, J.A., 2002. Mechanism of superoxide and hydrogen peroxide formation by fumarate reductase, succinate dehydrogenase, and aspartate oxidase. J. Biol. Chem. 277, 42563–42571.

Miyadera, H., Shiomi, K., Ui, H., Yamaguchi, Y., Masuma, R., Tomoda, H., Miyoshi, H., Osanai, A., Kita, K., Omura, S., 2003. Atpenins, potent and specific inhibitors of mitochondrial complex II (succinate–ubiquinone oxidoreductase). Proc. Natl. Acad. Sci. USA 100, 473–477.

Mohanty, J.G., Jaffe, J.S., Schulman, E.S., Raible, D.G., 1997. A highly sensitive fluorescent micro-assay of H2O2 release from activated human leukocytes using a dihydroxyphenoxazine derivative. J. Immunol. Methods 202, 133–141.

Muller, F.L., Liu, Y., Abdul-Ghani, M.A., Lustgarten, M.S., Bhattacharya, A., Jang, Y.C., Van Remmen, H., 2008. High rates of superoxide production in skeletal-muscle mitochondria respiring on both complex I- and complex II-linked substrates. Biochem. J. 409, 491–499.

Murphy, M.P., 2009. How mitochondria produce reactive oxygen species. Biochem. J. 417, 1–13.

Ni, Y., Zbuk, K.M., Sadler, T., Patocs, A., Lobo, G., Edelman, E., Platzer, P., Orloff, M.S., Waite, K.A., Eng, C., 2008. Germline mutations and variants in the succinate dehydrogenase genes in Cowden and Cowden-like syndromes. Am. J. Hum. Genet. 83, 261–268.

Paddenberg, R., Ishaq, B., Goldenberg, A., Faulhammer, P., Rose, F., Weissmann, N., Braun-Dullaeus, R.C., Kummer, W., 2003. Essential role of complex II of the respiratory chain in hypoxia-induced ROS generation in the pulmonary vasculature. Am. J. Physiol. Lung. Cell. Mol. Physiol. 284, L710–719.

Saruta, F., Hirawake, H., Takamiya, S., Ma, Y.C., Aoki, T., Sekimizu, K., Kojima, S., Kita, K., 1996. Cloning of a cDNA encoding the small subunit of cytochrome b558 (cybS) of mitochondrial fumarate reductase (complex II) from adult *Ascaris suum*. Biochim. Biophys. Acta. 1276, 1–5.

Saruta, F., Kuramochi, T., Nakamura, K., Takamiya, S., Yu, Y., Aoki, T., Sekimizu, K., Kojima, S., Kita, K., 1995. Stage-specific isoforms of complex II (succinate–ubiquinone oxidoreductase) in mitochondria from the parasitic nematode, *Ascaris suum*. J. Biol. Chem. 270, 928–932.

Senoo-Matsuda, N., Yasuda, K., Tsuda, M., Ohkubo, T., Yoshimura, S., Nakazawa, H., Hartman, P.S., Ishii, N., 2001. A defect in the cytochrome b large subunit in complex II causes both superoxide anion overproduction and abnormal energy metabolism in *Caenorhabditis elegans*. J. Biol. Chem. 276, 41553–41558.

Selak, M.A., Armour, S.M., MacKenzie, E.D., Boulahbel, H., Watson, D.G., Mansfield, K.D., Pan, Y., Simon, M.C., Thompson, C.B., Gottlieb, E., 2005. Succinate links TCA cycle dysfunction to oncogenesis by inhibiting HIF-alpha prolyl hydroxylase. Cancer Cell 7, 77–85.

Shinjyo, N., Kita, K., 2007. Relationship between reactive oxygen species and heme metabolism during the differentiation of Neuro2a cells. Biochem. Biophys. Res. Commun. 358, 130–135.

St-Pierre, J., Buckingham, J.A., Roebuck, S.J., Brand, M.D., 2002. Topology of superoxide production from different sites in the mitochondrial electron transport chain. J. Biol. Chem. 277, 44784–44790.

Sun, F., Huo, X., Zhai, Y., Wang, A., Xu, J., Su, D., Bartlam, M., Rao, Z., 2005. Crystal structure of mitochondrial respiratory membrane protein complex II. Cell 121, 1043–1057.

Szeto, S.S., Reinke, S.N., Sykes, B.D., Lemire, B.D., 2007. Ubiquinone-binding site mutations in the *Saccharomyces cerevisiae* succinate dehydrogenase generate superoxide and lead to the accumulation of succinate. J. Biol. Chem. 282, 27518–27526.

Takamiya, S., Furushima, R., Oya, H., 1986. Electron transfer complexes of Ascaris suum muscle mitochondria. II. Succinate–coenzyme Q reductase (complex II) associated with substrate-reducible cytochrome *b*558. Biochim. Biophys. Acta 848, 99–107.

Van Hellmond, J.J., van der Klei, A., van Weelden, S.W.H., Tielens, A.G.M., 2003. Biochemical and evolutionary aspects of anaerobically functioning bacteria. Phil. Trans. R. Soc. B. 358, 205–215.

Yamashita, T., Ino, T., Miyoshi, H., Sakamoto, K., Osanai, A., Nakamaru-Ogiso, E., Kita, K., 2004. Rhodoquinone reaction site of mitochondrial complex I, in parasitic helminth, *Ascaris suum*. Biochim. Biophys. Acta 1608, 97–103.

Yankovskaya, V., Horsefield, R., Tornroth, S., Luna-Chavez, C., Miyoshi, H., Leger, C., Byrne, B., Cecchini, G., Iwata, S., 2003. Architecture of succinate dehydrogenase and reactive oxygen species generation. Science 299, 700–704.

Zhang, L., Yu, L., Yu, C.A., 1998. Generation of superoxide anion by succinate–cytochrome c reductase from bovine heart mitochondria. J. Biol. Chem. 273, 33972–33976.

Zhao, Z., Rothery, R.A., Weiner, J.H., 2006. Effects of site-directed mutations in *Escherichia coli* succinate dehydrogenase on the enzyme activity and production of superoxide radicals. Biochem. Cell Biol. 84, 1013–1021.

nature immunology

Basophils contribute to T_H2-IgE responses *in vivo* via IL-4 production and presentation of peptide–MHC class II complexes to CD4$^+$ T cells

Tomohiro Yoshimoto[1,2], Koubun Yasuda[1,2], Hidehisa Tanaka[1,2], Masakiyo Nakahira[1,2], Yasutomo Imai[1,2], Yoshihiro Fujimori[3] & Kenji Nakanishi[1,2]

Basophils express major histocompatibility complex class II, CD80 and CD86 and produce interleukin 4 (IL-4) in various conditions. Here we show that when incubated with IL-3 and antigen or complexes of antigen and immunoglobulin E (IgE), basophils internalized, processed and presented antigen as complexes of peptide and major histocompatibility complex class II and produced IL-4. Intravenous administration of ovalbumin-pulsed basophils into naive mice 'preferentially' induced the development of naive ovalbumin-specific CD4$^+$ T cells into T helper type 2 (T_H2) cells. Mice immunized in this way, when challenged by intravenous administration of ovalbumin, promptly produced ovalbumin-specific IgG1 and IgE. Finally, intravenous administration of IgE complexes rapidly induced T_H2 cells only in the presence of endogenous basophils, which suggests that basophils are potent antigen-presenting cells that 'preferentially' augment T_H2-IgE responses by capturing IgE complex.

Atopic people, after repeated exposure to a particular antigen, develop strong T helper type 2 (T_H2) responses and produce immunoglobulin E (IgE). IgE then sensitizes mast cells and basophils by binding to their FcεRI receptor (A000543)[1–3]. Subsequent exposure to the same antigen activates the mast cells and basophils to secrete the chemical mediators, cytokines and chemokines that result in the pathological reactions of immediate hypersensitivity. IgE is a unique antibody that upregulates expression of FcεRI on mast cells and basophils, thereby providing a mechanism for the amplification of IgE-mediated reactions[4,5]. Indeed, a strong positive correlation exists between FcεRI expression on basophils and IgE titers in human peripheral blood[6]. Furthermore, as with the inhalation of ragweed pollen, low antigen dose without adjuvant can induce IgE production, which suggests that there is an amplification loop for IgE production *in vivo*. Thus, once atopic people begin to produce IgE, they develop progressive allergic inflammation by increasing production of IgE and expression of FcεRI on effector cells.

Basophils and mast cells are important effector cells in IgE-mediated allergic inflammation[1–3]. Progenitors of mast cells in the bone marrow migrate to the peripheral tissues as immature cells and undergo differentiation *in situ*[1,7]. Thus, normally, mature mast cells are not found in the circulation. In contrast, basophils are rare circulating granulocytes that originate from progenitors in the bone marrow. Basophils constitute less than 1% of blood leukocytes and are normally not present in tissues. However, they may be recruited to some inflammatory sites where antigen is present and contribute to immediate hypersensitivity reactions[8–11]. Studies also suggest that basophils induce IgE-mediated chronic allergic inflammation and IgG1-mediated systemic anaphylactic shock[12–14]. Thus, basophils are primary effector cells in allergic disorders.

However, some lines of evidence have shown that these cells are important regulators of T_H2 responses *in vivo*, particularly in helminth-infected mice[15–20]. In general, the entry of an invading pathogen triggers recognition by dendritic cells (DCs) through Toll-like receptors (TLRs) and their subsequent maturation to express costimulatory molecules and produce interleukin 12 (IL-12) and IL-18, which favor T_H1 responses[21–24]. In contrast, infection with helminths strongly induces T_H2 cells and the proliferation of basophils in the spleens and livers of host mice[18], which suggests a contribution of basophils to the induction and/or augmentation of T_H2 responses. The development of naive CD4$^+$ T cells into T_H2 cells is dependent on IL-4 (A001262) in the milieu[25]. However, the nature of cells that produce 'early' IL-4, required for the development of naive CD4$^+$ T cells into T_H2 cells, remains unknown[26]. IL-18 with IL-3 or IL-33 with IL-3 strongly induces basophils but not mast cells to produce both IL-4 and IL-13 *in vitro*[27,28], which suggests basophils are involved in the induction of T_H2 cells by functioning as early IL-4-producing cells. Other published studies have also indicated that basophils are critically involved in T_H2 responses by their unique ability to produce early IL-4 and thymic stromal lymphopoietin in response to papain or

[1]Department of Immunology and Medical Zoology, Hyogo College of Medicine, Nishinomiya, Hyogo, Japan. [2]Collaborative Development of Innovative Seeds, Japan Science and Technology Corporation, Saitama, Japan. [3]Laboratory of Cell Transplantation, Institute for Advanced Medical Sciences, Hyogo College of Medicine, Nishinomiya, Hyogo, Japan. Correspondence should be addressed to K.N. (nakaken@hyo-med.ac.jp).

Received 16 December 2008; accepted 14 April 2009; published online 24 May 2009; doi:10.1038/ni.1737

bromelain[29]. Thus, here we studied the mechanism that accounts for the induction and progression of allergic response by positive feedback loops between IgE and basophils *in vivo*. We demonstrate the contribution of basophils to the T_H2-IgE response *in vitro* and *in vivo* through the production of IL-4 and presentation of complexes of peptide and major histocompatibility complex (MHC) class II to naive $CD4^+$ T cells, in contrast to the T_H1 cell–inducing action of DCs.

RESULTS

Basophils induce the development of T_H2 cells *in vitro*

We first examined the ability of splenic basophils from naive mice and mice infected with *Strongyloides venezuelensis*[30] to produce T_H2 cytokines and to induce the development of naive $CD4^+$ cells into T_H2 cells *in vitro*. We prepared non–T cell, non–B cell fractions from spleens of naive mice and infected mice and determined the proportion of $Fc\varepsilon RI^+c\text{-}Kit^-$ cells (basophils) in those fractions. Non–T cell, non–B cell fractions from spleens of naive mice contained 0.20% $Fc\varepsilon RI^+c\text{-}Kit^-$ cells, whereas those from *S. venezuelensis*–infected mice had a much greater proportion of these cells (5.84%; **Fig. 1a**), as reported for mice infected with *Nippostrrongylus brasiliensis*[18]. Furthermore, *S. venezuelensis*–infected mice had a greater proportion of $Fc\varepsilon RI^+c\text{-}Kit^+$ cells (mast cells) in those fractions (0.02% in naive mice compared with 0.39% in infected mice). We purified basophils from the spleens of naive mice and infected mice (**Fig. 1a**) and examined their production of cytokines and expression of MHC class II molecules. Splenic basophils from infected mice cultured for 24 h with IL-3 produced large amounts of IL-4, IL-6 and IL-13, whereas those from naive mice produced small amounts of these T_H2 cytokines, although both types of basophils produced similar amounts of IL-10 (**Fig. 1b**). However, the production of IL-17A, interferon-γ (IFN-γ) and tumor necrosis factor was low (**Fig. 1b**). As reported before[27], basophils from infected mice were able to produce IL-4 without IL-3 stimulation, whereas basophils from naive mice did not produce IL-4 in the absence of IL-3 *in vitro* (**Supplementary Table 1** online), which suggests that basophils in infected mice gain the ability to produce substantial IL-4 even in the absence of IL-3. Flow cytometry of basophils from naive mice and infected mice showed that they had abundant and comparable expression of MHC class II (**Fig. 1c**). Peripheral blood basophils from naive mice also expressed MHC class II molecules (**Fig. 1c**).

As splenic basophils from infected mice expressed MHC class II and had the potential to produce substantial IL-4, IL-6 and IL-13 in cultures containing IL-3, we next examined their ability to induce ovalbumin (OVA)-specific naive $CD4^+$ T cells to develop into T_H2 cells *in vitro* in the presence of OVA peptide (amino acids 323–339 (OVA(323–339)), IL-2 and IL-3 without IL-4 ('neutral' culture conditions). We simultaneously cultured naive $CD4^+$ T cells with conventional antigen-presenting cells (APCs; T cell–depleted splenic cell samples (ΔT-spleen cells)) in the presence of OVA(323–339) in neutral conditions (**Fig. 1d**). Splenic basophils from *S. venezuelensis*–infected mice showed a notable ability to induce naive $CD4^+$ T cells to develop into T_H2 cells (**Fig. 1d**). In contrast, as reported elsewhere[25], conventional APCs failed to induce T_H2 cells in these neutral conditions, although both types of APC strongly induced the development of T_H2 cells in T_H2 conditions (**Fig. 1d**). We found that like typical T_H2 cells that developed in T_H2 conditions

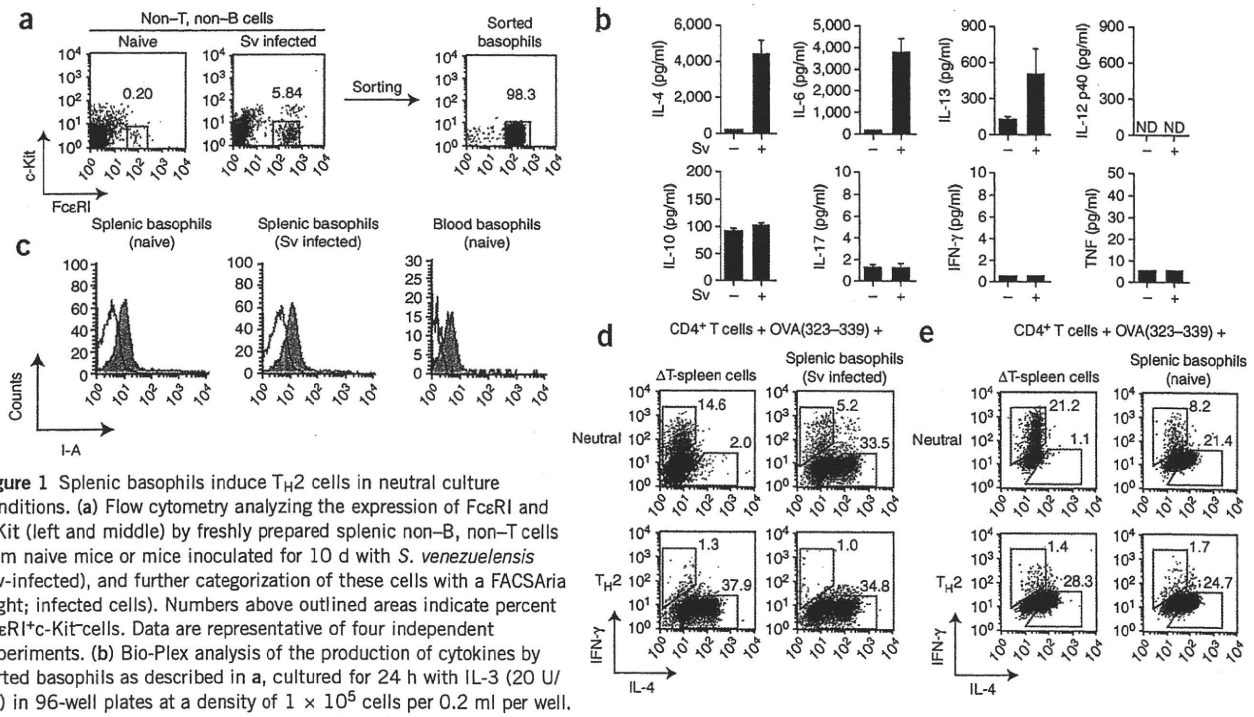

Figure 1 Splenic basophils induce T_H2 cells in neutral culture conditions. (**a**) Flow cytometry analyzing the expression of FcεRI and c-Kit (left and middle) by freshly prepared splenic non–B, non–T cells from naive mice or mice inoculated for 10 d with *S. venezuelensis* (Sv-infected), and further categorization of these cells with a FACSAria (right; infected cells). Numbers above outlined areas indicate percent $Fc\varepsilon RI^+c\text{-}Kit^-$cells. Data are representative of four independent experiments. (**b**) Bio-Plex analysis of the production of cytokines by sorted basophils as described in **a**, cultured for 24 h with IL-3 (20 U/ml) in 96-well plates at a density of 1×10^5 cells per 0.2 ml per well. ND, not detected. Data are representative of two independent experiments (mean and s.e.m. of three mice). (**c**) Flow cytometry of sorted splenic basophils from naive mice (left) or *S. venezuelensis*–infected mice (middle), stained for MHC class II molecules (I-A), and of peripheral blood mononuclear cells from naive mice, stained for MHC class II molecules and gated on $Fc\varepsilon RI^+DX5^+B220^-CD3^-$ cells (right). Filled histograms, markers; lines, unstained cells. Data are representative of two independent experiments with five mice. (**d**,**e**) Flow cytometry analyzing cytosolic IL-4 and IFN-γ in naive splenic DO11.10 $CD4^+CD62L^+$ T cells (1×10^5 cells per ml) stimulated for 7 d in 48-well plates with IL-2 (100 pM), IL-3 (20 U/ml) and OVA(323–339) (1 μM) in the presence of irradiated BALB/c ΔT-spleen cells or irradiated splenic basophils (5×10^5 cells per ml each) from *S. venezuelensis*–infected mice (**d**) or naive mice (**e**), with (T_H2) or without (Neutral) IL-4 (1,000 U/ml), then washed and recultured for 4 h with the phorbol ester PMA (50 ng/ml) plus ionomycin (0.5 μg/ml). Numbers adjacent to outlined areas indicate percent $IL\text{-}4^+$ or $IFN\text{-}\gamma^+$ cells gated on $CD4^+$ T cells. Data are representative of three independent experiments.

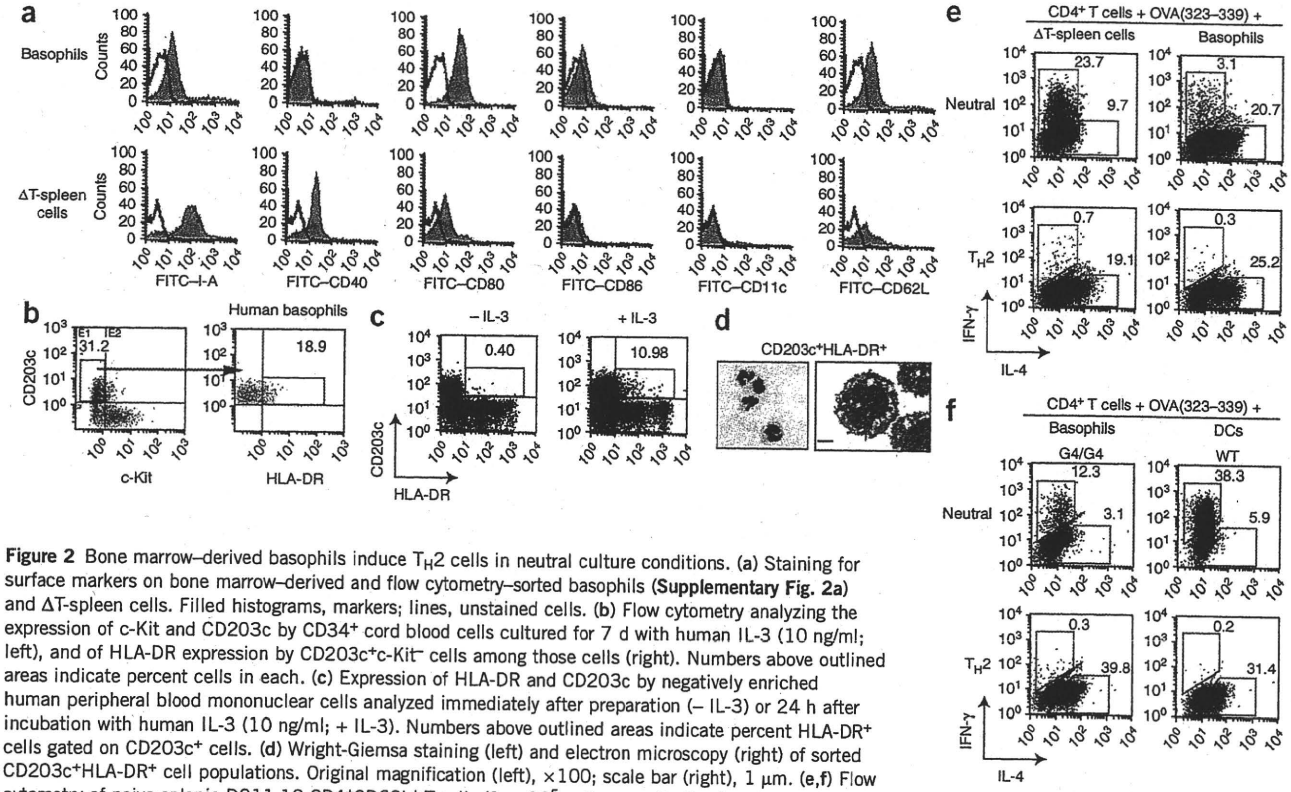

Figure 2 Bone marrow–derived basophils induce T_H2 cells in neutral culture conditions. (**a**) Staining for surface markers on bone marrow–derived and flow cytometry–sorted basophils (**Supplementary Fig. 2a**) and ΔT-spleen cells. Filled histograms, markers; lines, unstained cells. (**b**) Flow cytometry analyzing the expression of c-Kit and CD203c by $CD34^+$ cord blood cells cultured for 7 d with human IL-3 (10 ng/ml; left), and of HLA-DR expression by $CD203c^+c\text{-}Kit^-$ cells among those cells (right). Numbers above outlined areas indicate percent cells in each. (**c**) Expression of HLA-DR and CD203c by negatively enriched human peripheral blood mononuclear cells analyzed immediately after preparation (– IL-3) or 24 h after incubation with human IL-3 (10 ng/ml; + IL-3). Numbers above outlined areas indicate percent $HLA\text{-}DR^+$ cells gated on $CD203c^+$ cells. (**d**) Wright-Giemsa staining (left) and electron microscopy (right) of sorted $CD203c^+HLA\text{-}DR^+$ cell populations. Original magnification (left), ×100; scale bar (right), 1 μm. (**e,f**) Flow cytometry of naive splenic DO11.10 $CD4^+CD62L^+$ T cells (1×10^5 cells per ml) stimulated and analyzed as described in **Figure 1d**, with irradiated ΔT-spleen cells, purified bone marrow–derived wild-type (WT) or IL-4-deficient (G4/G4) basophils or wild-type splenic DCs as APCs. Data are representative of three or four independent experiments.

(**Fig. 1d**), T_H2 cells that developed after culture of naive $CD4^+$ T cells together with basophils in neutral culture conditions (**Fig. 1d**) produced IL-4, IL-5, IL-6, IL-10 and IL-13 (**Supplementary Fig. 1a** online), which suggested that these were true T_H2-polarized cells.

Next we assessed whether basophils from naive mice were also able to induce the development of T_H2 cells *in vitro*. We found that those splenic basophils also had a potent T_H2 cell–inducing function (**Fig. 1e**). As expected, some of the T_H2 cells induced in neutral conditions (**Fig. 1d**) expressed T_H2 cell marker IL-33Rα[31] (**Supplementary Fig. 1b**) and increased their production of T_H2 cytokines other than IL-4 when challenged with antigen plus IL-33 *in vitro* (**Supplementary Fig. 1c**).

Bone marrow basophils induce T_H2 cells *in vitro*

We next examined the ability of highly purified bone marrow basophils (**Supplementary Fig. 2a** online), devoid of other potential APCs, to induce T_H2 cell development *in vitro*. We first examined their expression of MHC class II molecules and the costimulatory molecules CD80 and CD86 (**Fig. 2a**). We simultaneously examined the expression of these molecules by conventional APCs. Bone marrow–derived basophils and conventional APCs expressed MHC class II, CD80 and CD86 but not CD11c. Basophils also expressed the lymph node–homing molecule CD62L, which suggested their potential to enter into lymphoid tissues[32]. As reported before[33], a fraction of human immature basophils ($CD203c^+c\text{-}Kit^-$) derived from cord blood expressed HLA-DR (18.9%; **Fig. 2b**). Although immature basophils decrease their expression of HLA-DR after maturation[33], we found mature peripheral blood basophils re-expressed HLA-DR after being cultured for 24 h with IL-3 (**Fig. 2c,d** and **Supplementary Fig. 2b**). In contrast, mouse peripheral basophils that expressed MHC class II failed to increase this expression in IL-3-containing medium (**Supplementary Fig. 2c**).

We compared the ability of conventional APCs and basophils to induce T_H2 cell development *in vitro* in neutral and T_H2 conditions (**Fig. 2e**). In the absence of any other APC, bone marrow–derived basophils were able to induce naive $CD4^+$ T cells to develop into T_H2 cells in neutral culture conditions as described above (20.7%), whereas conventional APCs induced T_H2 cells only in T_H2 conditions (**Fig. 2e**). Additional IL-4 stimulation (T_H2 conditions) resulted in an only modestly enhanced capacity of basophils to induce T_H2 cell development (25.2%; **Fig. 2e**), which suggests that bone marrow basophils produce sufficient IL-4 for maximum development of T_H2 cells. Indeed, basophils from IL-4-deficient G4/G4 mice[34] could not induce the development of T_H2 cells (3.1%) in neutral conditions (**Fig. 2f**). However, such IL-4-deficeint basophils did induce T_H2 cells in T_H2 conditions (39.8%), which allowed us to conclude that endogenous IL-4 from basophils was essential for the development of naive $CD4^+$ T cells into T_H2 cells. As reported elsewhere[25], splenic DCs induced T_H2 cells only in T_H2 cell–inducing conditions (**Fig. 2f**).

Basophils pulsed with antigen-IgE complexes are potent APCs

It was important to demonstrate the ability of basophils to take up and process OVA protein into OVA(323–339). We used 2,4-dinitrophenyl (DNP)-conjugated OVA (DNP-OVA) instead of OVA protein in this experiment and subsequent experiments, as DNP-OVA can also yield OVA(323–339) after processing. We were able to induce OVA-specific

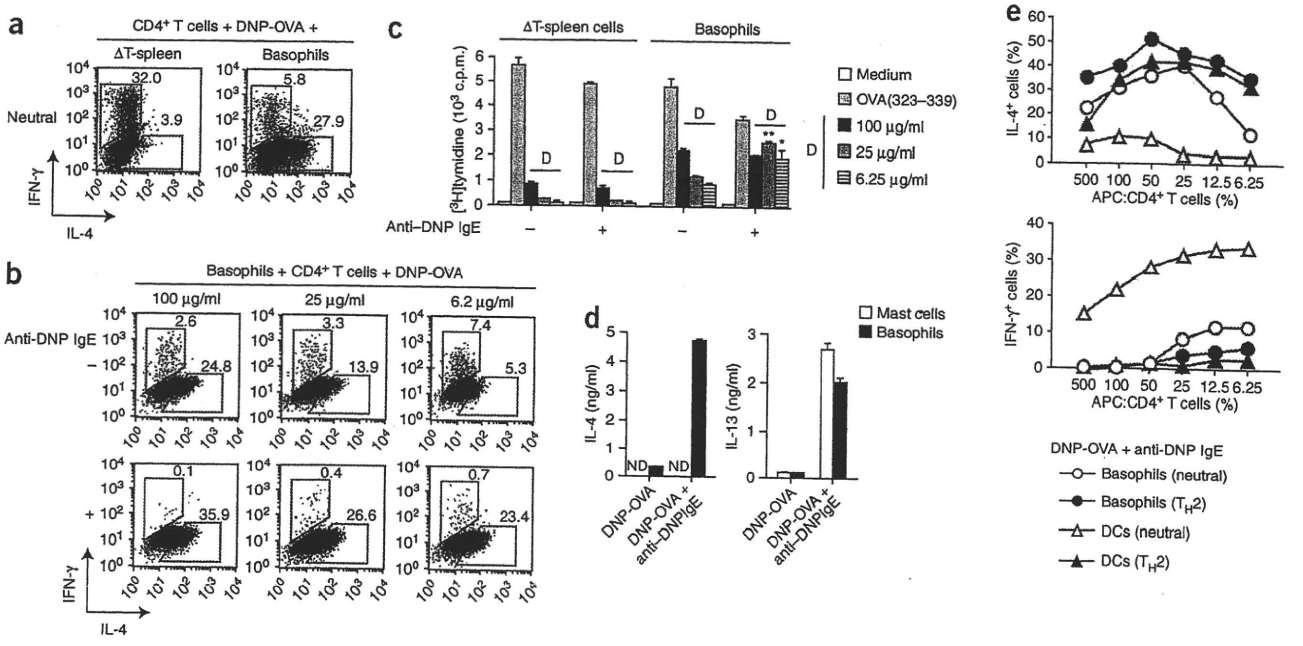

Figure 3 IgE complex enhances uptake of OVA by basophils. (**a**,**b**) Flow cytometry (as described in **Fig. 1d**) of naive splenic DO11.10 CD4+CD62L+ T cells (1×10^5 cells per ml) stimulated for 7 d with IL-2, IL-3 and DNP-OVA (100 μg/ml; **a**), or DNP-OVA (6.25–100 μg/ml) with or without IgE anti-DNP (10 μg/ml; **b**) in the presence of irradiated ΔT-spleen cells or bone marrow–derived basophils (5×10^5 cells per ml each). (**c**) Proliferative responses of naive splenic DO11.10 CD4+CD62L+ T cells (5×10^4 cells per 0.2 ml per well) cultured for 4 d in 96-well plates with OVA(323–339) (1 μM) or DNP-OVA (D; 6.25–100 μg/ml; in key) with or without IgE anti-DNP (10 μg/ml). *, $P < 0.05$ and **, $P < 0.005$, versus cells without anti–DNP IgE (Student's *t*-test). (**d**) Cytokine production by bone marrow–derived basophils or mast cells (5×10^5 cells per ml each) stimulated for 16 h in 48-well plates with IL-3 and DNP-OVA (100 μg/ml) with or without IgE anti-DNP (10 μg/ml). (**e**) Flow cytometry (as described in **Fig. 1d**) of naive splenic DO11.10 CD4+CD62L+ T cells (1×10^5 cells per ml) stimulated for 7 d with IL-2, IL-3, DNP-OVA (100 μg /ml) and IgE anti-DNP (10 μg /ml) in the presence of various numbers (6.25×10^3 to 5×10^5 cells per ml) of irradiated splenic DCs or bone marrow basophils with IL-4 (T_H2) or without IL-4 (Neutral). Data are representative of four (**a**–**d**) or two (**e**) independent experiments (mean and s.e.m. in **c**,**d**).

T_H2 cells by culturing naive CD4+ T cells with basophils in the presence of IL-2, IL-3 and DNP-OVA (100 μg/ml) without IL-4 (**Fig. 3a**). Again, conventional APCs failed to induce the development of T_H2 cell in these neutral culture conditions (**Fig. 3a**). Thus, basophils are able to process DNP-OVA into OVA(323–339) and to display peptide fragment in association with MHC class II and to produce IL-4.

It was also important to demonstrate the unique potential of basophils to increase their capacity to act as APCs when pulsed with antigen in the presence of antigen-specific IgE. Thus, we pulsed basophils with various doses of DNP-OVA in the presence or absence of monoclonal antibody to DNP (IgE anti-DNP; **Fig. 3b**). Basophils pulsed with a low dose (6.2 μg/ml) of DNP-OVA modestly induced T_H2 cells (5.3%), whereas pulsation with a higher dose (100 μg/ml) of DNP-OVA resulted in a higher proportion of 24.8%. The addition of IgE anti-DNP resulted in much higher proportions, particularly at lower concentrations of DNP-OVA (no IgE anti-DNP, 5.3%, 13.9% and 24.8%, versus with IgE anti-DNP, 23.4% 26.6% and 35.9%, for 6.2 μg/ml, 25 μg/ml and 100 μg/ml of DNP-OVA, respectively; **Fig. 3b**). Thus, the enhancing effect of IgE anti-DNP on basophil-induced T_H2 cell development was most apparent when basophils were pulsed with low concentrations of DNP-OVA.

We next examined whether IgE anti-DNP could enhance the capacity of conventional APCs to function as APCs. Thus, we cultured OVA(323–339)-specific T cells with conventional APCs or basophils in the presence of OVA(323–339) or DNP-OVA with or without IgE anti-DNP. Basophils pulsed with DNP-OVA in the presence of IgE anti-DNP had a significantly greater capacity to induce the proliferation of OVA–specific T cells (**Fig. 3c**). In contrast, conventional APCs pulsed with DNP-OVA in the presence of IgE anti-DNP did not have a greater capacity to induce T cell proliferation (**Fig. 3c**). These results suggest that basophils, taking advantage of their expression of FcεRI, might efficiently take up low doses of antigen in an IgE-dependent way.

As reported before[35], basophils had a much greater capacity to produce IL-4 and IL-13 after being pulsed with DNP-OVA in the presence of IgE anti-DNP (**Fig. 3d**). In contrast, mast cells pulsed with DNP-OVA–IgE anti-DNP immune complexes produced only IL-13, not IL-4 (**Fig. 3d**). We prepared basophils and mast cells from bone marrow cells cultured for 14 d with IL-3 (**Supplementary Fig. 2a**). We stimulated those cells with mixture of DNP-OVA and IgE anti-DNP. Mast cells prepared from bone marrow cells cultured for 4–6 weeks in medium conditioned by mouse leukemic WEHI-3 cells (containing IL-3) are reported to produce IL-4 after sequential IgE anti-DNP sensitization and subsequent DNP-protein challenge[36]. In addition to that unique function, we found that only basophils, when stimulated with IL-3 plus IL-18, IL-33, peptidoglycan or lipopolysaccharide, produced both IL-4 and IL-13 (**Supplementary Fig. 3a,b** online). Thus, basophils became producers of large amounts of IL-4 in *S. venezuelensis*–infected mice (**Fig. 1b**) or *in vitro* when stimulated with DNP-OVA–anti-DNP IgE in the presence of IL-3. Next we compared the APC activity of basophils and sorted CD11c+ splenic DCs[37] by changing the ratio of APCs to naive CD4+ T cells. Again, only basophils 'preferentially' induced the development of T_H2 cells in